DOKUZ EYLÜL UNIVERSITY

GRADUATE SCHOOL OF NATURAL AND APPLIED SCIENCES

DEVELOPMENT OF AN ACOUSTIC METAMATERIAL HAVING HIGH SOUND ABSORPTION FOR LOW FREQUENCY NOISE

by

Tuba BAYGÜN

July, 2019

İZMİR

DEVELOPMENT OF AN ACOUSTIC METAMATERIAL HAVING HIGH SOUND ABSORPTION FOR LOW FREQUENCY NOISE

A Thesis Submitted to the
Graduate School of Natural and Applied Sciences of Dokuz Eylül University
In Partial Fulfillment of the Requirements for the Degree of Master of Science
in Mechanical Engineering, Machine Theory and Dynamics Program

by
Tuba BAYGÜN

July, 2019
İZMİR

M.Sc. THESIS EXAMINATION RESULT FORM

We have read the thesis entitled **"DEVELOPMENT OF AN ACOUSTIC METAMATERIAL HAVING HIGH SOUND ABSORPTION FOR LOW FREQUENCY NOISE"** completed by **TUBA BAYGÜN** under supervision of **ASSOC. PROF. DR. ABDULLAH SEÇGİN** and we certify that in our opinion it is fully adequate, in scope and in quality, as a thesis for the degree of Master of Science.

Assoc. Prof. Dr. Abdullah SEÇGİN

Supervisor

Prof. Dr. A. Saide SARIGÜL
(Jury Member)

Doç. Dr. Mehmet SARIKANAT
(Jury Member)

Prof. Dr. Kadriye ERTEKİN
Director
Graduate School of Natural and Applied Sciences

ACKNOWLEDGMENTS

I would like to express my deep appreciation to my thesis advisor Assoc. Prof. Dr. Abdullah SEÇGİN for all his time, effort and patience. His guidance and critical suggestions helped me to finish this thesis.

I would also like thanks to Res. Ass. Murat KARA and my friend Çağrı Gökhan AKYOL.

Finally, my special thanks go to my parents for their support in my entire master education.

Tuba BAYGÜN

DEVELOPMENT OF AN ACOUSTIC METAMATERIAL HAVING HIGH SOUND ABSORPTION FOR LOW FREQUENCY NOISE

ABSTRACT

Machinery noise is an important problem for human health, environment, and efficiency and longevity of machines. Besides that, the insulation of noise is a legal requirement; it is also of importance in buildings, vehicles, aerospace structures and pipeline systems for better comfort and quality conditions. Conventional passive noise insulations are limited in practical use, since the mass law dictating that the thickness of the insulation material must be comparable in size with the propagation wavelength which makes them inefficient. Recently an "acoustic metamaterial" concept has emerged and proved itself that it may break the mass law in a certain frequencies or frequency bands. Acoustic metamaterials (AMMs) are usually periodic sub-wavelength artificial structures exhibiting extraordinary material properties, such as negative effective mass density and effective bulk modulus.

This thesis concerns with designing of AMMs for suppressing low frequency noise with providing higher absorption. For this purpose, several different kinds of AMMs are designed for acoustic transmission lines and for panel absorbers. Acoustic performance parameters such as sound transmission, reflection and absorption coefficients are obtained to exhibit performances of the designed materials. They are determined by transfer matrix method and finite element method for acoustic transmission lines. All analyses take visco-thermal effects into account and metamaterial properties are characterized based on effective medium theory. For panel absorber AMMs, acoustic performance parameters are experimentally determined by impedance tube measurements.

Keywords: Acoustic metamaterials, low frequency absorption, effective medium theory, noise insulation materials, transfer matrix method, finite element method

DÜŞÜK FREKANS GÜRÜLTÜSÜ İÇİN YÜKSEK SES YUTUMUNA SAHİP BİR AKUSTİK METAMALZEME GELİŞTİRİLMESİ

ÖZ

Makine gürültüsü, insan sağlığı, çevre ve makinelerin verimlilik ve uzun ömürlülüğü için önemli bir sorundur. Bunun yanında, ses yalıtımı yasal bir gerekliliktir; binalarda, araçlarda, havacılık yapılarında ve boru hattı sistemlerinde daha iyi konfor ve kalite koşulları için de önemlidir. Geleneksel pasif ses yalıtımı pratik kullanımda sınırlıdır. Çünkü yalıtım malzemesinin kalınlığının, yayınımın dalga boyu ile karşılaştırılabilir olması gerektiğini belirleyen kütle yasası, onları verimsiz kılar. Son yılarda ortaya çıkan "akustik metamalzeme" kavramı belirli bir frekans veya frekans bandında kütle yasasını kırabileceğini kanıtlamıştır. Akustik metamalzemeler (AMM'ler) negatif etkin kütle yoğunluğu ve etkin Bulk modülü gibi olağandışı malzeme özellikleri sergileyen genellikle periyodik alt dalga boyuna sahip yapay yapılardır.

Bu tez, düşük frekanslı gürültü azaltımı için yüksek yutum sağlayan AMM'lerin tasarlanması ile ilgilenmektedir. Bu amaçla, akustik iletim hatları ve panel tip yutucular için çeşitli AMM'ler tasarlanmıştır. Tasarlanan malzemelerin performanslarını ortaya koymak amacıyla ses iletim, yansıma ve yutma katsayıları gibi akustik performans parametreleri elde edilmiştir. Akustik iletim hatları için bu parametreler, transfer matrisi yöntemi ve sonlu elemanlar yöntemi ile belirlenmiştir. Tüm analizlerde visko-termal etkiler hesaba katılmış ve metamalzeme özellikleri, etkin ortam teorisine dayanarak karakterize edilmiştir. Panel tip yutucu AMM'ler için, akustik performans parametreleri deneysel olarak empedans tüpü ölçümleriyle belirlenmiştir.

Anahtar Kelimeler: Akustik metamalzeme, düşük frekans yutumu, etkin ortam teorisi, ses yalıtım malzemeleri, transfer matris yöntemi, sonlu eleman yöntemi

CONTENTS

LIST OF FIGURES

LIST OF TABLES

Page

CHAPTER ONE
INTRODUCTION

1.1 Motivation and Objective of the Thesis

Noise caused by a machine is an important problem for not only human health or environment but also for the efficiency and longevity of machines and their parts. Because the noise emitted by a machine warns that there may be unbalanced forces causing vibration, and thus influencing the machine performance. Therefore noise insulation is a requirement, and is of importance in buildings, vehicles, aerospace structures, and pipeline systems. Generally, the insulation is realized by three different ways; active, passive and adaptive isolation. Active isolation aims for reducing noise at the source itself. However passive isolation attempts to reduce to noise by using insulation materials placed between source and receiver. Adaptive isolation is a kind of passive isolation which creates a sound wave with the same frequency, but in the opposite phase emitted in the noisy medium. Since the first and the third isolation techniques are relatively hard and expensive in applications, passive isolation is the most preferred way in practice. However, since the mass law (see Zone II in Fig. 1.1) dictates that the thickness of the insulation material must be comparable in size with the propagation wavelength, they are not so efficient and rather limited in use of low frequency noise insulation.

Recently a concept called “metamaterial” has attracted by the researchers due to the fact that they may break the mass law in certain frequencies. In general definition, metamaterials (MMs) are artificial structures (not found in nature), made of periodic or non-periodic, sub-wavelength units in which the presence of local resonances leads to unusual material properties. “Sub-wavelength unit” expression here states that the characteristic length of unit cell is much smaller than the wavelength of the propagation in the medium. The word "meta" means "beyond" in Greek. In this context, although there is no compromise on the definition of metamaterials, they are generally defined as the material exhibiting extraordinary material behaviour beyond the physical properties of conventional isolation materials, such as permeability, permittivity in electro-magnetic materials (EMMs), and mass density, Bulk modulus (inverse of compressibility) in AMMs.

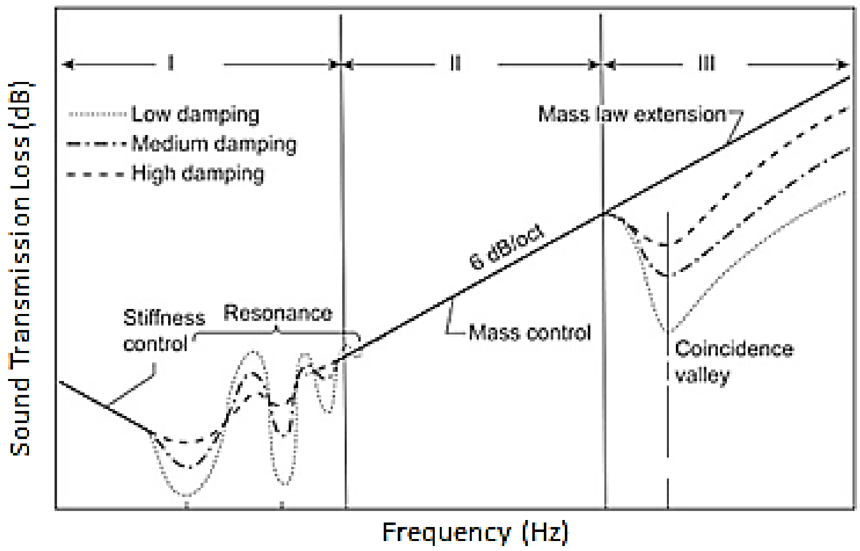

Figure 1.1 Sound transmission diagram of a typical structure (Peng, 2017)

By motivated from the aforementioned issues; this thesis concerns with designing of such acoustic metamaterials (AMMs) for suppressing low frequency noise with a high absorption at some certain frequencies. In the thesis, several different kinds of AMMs are designed for the acoustic transmission lines and panel type absorbers. Acoustic performance parameters such as transmission, reflection and absorption coefficients are selected to exhibit the performance characteristics of the designed AMMs. For the quantification of material properties by means of homogenous parameters, effective medium theory is applied by using an inverse method based on transfer matrix method (TMM). One may also find the details of a retrieving effective medium parameter procedure in the thesis. Determination of acoustic performance parameters are realized by finite element method (FEM) and TMM for acoustic transmission lines. For panel type absorbers, performance parameters are experimentally computed by using impedance tube kit. For more realistic analyses both TMM and FEM analyses include visco-thermal effects. The thesis also briefly presents analytical visco-thermal models and includes a simple but informative comparison between these v-t models. Following sections of this Chapter involve a comprehensive literature survey on AMMs and thesis organization.

1.2 Literature Summary

In recent decade, a concept called acoustic metamaterial (AMM) inspired from electromagnetic metamaterials (EMMs) was emerged. Although it was not named as "metamaterial" in those years, the first theoretical study on metamaterials (MMs) was made by Veselago (2005). He stated that phase and group velocities may be in opposite direction to each other in an electromagnetic environment. This promised that the EMMs have a great potential for scientific research and industrial applications such as cloaking, super lensing, focusing etc.

The theoretical fundamentals of AMMs are based on the available information on electromagnetic metamaterials. AMMs are artificial structures made of periodic or non-periodic sub-wavelength units. These units can exhibit negative effective material properties. Some applications which have been studied on EMMs, have also been performed for AMMs (Ambati, Fang, Sun, & Zhang, 2007; Ying Cheng, Yang, Xu, & Liu, 2008; Cummer et al., 2008; Farhat, Guenneau, Enoch, & Movchan, 2009; Guenneau, Movchan, Pétursson, & Anantha Ramakrishna, 2007; Popa, Zigoneanu, & Cummer, 2011). Ma and Sheng (2016), Haberman and Guild (2016), Cummer et.al (2016) and Haberman and Norris (2016) presented very informative review papers on abilities of AMMs. However, it will be useful here to study some of the researches which are directly related to the objective of the present thesis.

There are numerous researches on AMMs in the last 20 years for various purposes. Although there is no compromise in the classification of AMM, they are generally categorized in two ways according to negativity and cellular characteristics. An example for the classification of AMMs can be seen in Table 1.1.

Table 1.1 Classification of acoustic metamaterials (Seçgin & Baygün, 2019b)

Negativity Characteristics	Cellular Characteristics
Single Negative (SNG)	Phononic Crystal (PC)
Double Negative (DNG)	Locally Resonant Sonic based
Near Zero (NZ)	Acoustic Cavity based
	Membrane based
	Hybrid

It should be noted that the issue of whether Phononic Crystals (PCs) (resembling photonic crystals in optic) are belong to AMMs is arguable. PCs are also artificial, periodically arranged small scatterers embedded in a medium. They may create Bragg type band gap at which sound wave transmission is prohibited. Zhang and Liu (2004) showed that acoustic waves in two-dimensional PCs may have a negative refractive index, such as electromagnetic waves. In their study, they designed a super lens and demonstrated the super focusing behaviour of the electromagnetic waves in photonic crystals for acoustic waves. A comprehensive overview on PCs can be found in Ref. (Hussein, Leamy, & Ruzzene, 2014). One can also refer to an edited book of Deymier (2013) for PCs and AMMs. However, due to the small size of PCs, they are generally useful in the manipulation of sound wave at high frequencies.

At this point, it will be appropriate to discuss other types of AMM studies which are summarized below according to AMMs' negativity/cellular properties.

Liu et. al. (2000) manufactured metal spheres coated with elastic silicon rubbers exhibiting local resonance frequency which is several times smaller than Bragg frequency. This study is a first transition from PC to "locally resonant sonic material (LRSM)". Sheng et al. (2003) followed the work of creating local resonances by coated PCs. Hirsekorn et al. (2004) performed numerical simulations on LRSMs. Movchan and Guennau (2004) used split ring resonators to control localized low frequencies. Zhao et al. (2005) increased the Bragg bandwidth displayed by PCs by interaction between active homogeneous media and solid body resonances. Lazarov and Jensen (2007) used spring-mass oscillators to achieve band gap close to local resonance. Huang et.al (2009) performed mass in mass lattice model to achieve the same purpose. Zhou and Hu (2009) constructed and analytical model for effective mass density, bulk and shear modulus of elastic metamaterials composed of coated spheres embedded in a host matrix similar to the model of Liu et. al (2000).

Fang et al. (2006) designed an ultrasonic metamaterial with a negative compressibility consisting of a Helmholtz resonator series, and showed that phase and group velocity could be in opposite direction. Hu et al. (2008) obtained analytically the effective medium parameters of a Helmholtz resonator in the fluid and supported the aforementioned findings of Fang et al. (2006). Lee et al. (2009b) created a negative compressibility by developing a different metamaterial with side holes in a pipeline. With this material, they have shown analytically and experimentally that they may prohibit sound transmission below 450 Hz. Lee et al. (2009a) developed another metamaterial with a negative effective density at resonance frequencies of membranes by placing very thin membranes in a pipe transmission line.

Yang et al. (2008) designed a different metamaterial by placing small masses on very thin membranes showing negative effective density which can be adjusted to desired frequencies. They confirmed their results by experimental studies. Yao et al. (2008) showed experimentally that negative density can be achieved by oscillators consisting of a large number of small mass and spring systems.

Beside that several simultaneously double negative metamaterials were designed including zero and /or negative mass and /or negative elasticity (Bongard, Lissek, & Mosig, 2010; Y. Cheng, Xu, & Liu, 2008; Ding, Liu, Qiu, & Shi, 2007; Li & Chan, 2004). Li and Chan (2004) mathematically proved on an example of soft rubber in water that Veselego's double negativity is also possible in AMMs (Veselago, 2005).

Recent studies conducted on so-called hybrid metamaterials (Y. Chen & Wang, 2014; Croënne, Lee, Hu, & Page, 2011; Krushynska, Miniaci, Bosia, & Pugno, 2017). In these works, the main idea to couple local resonance and Bragg band gaps to widen and enhance. Chen and Wang (2014) showed by numerical simulations that the correlative effect of Bragg scattering and local resonances increased the wave filtering property.

Here being more specific to the objective of the thesis, it is convenient to discuss transmission line problems handled by acoustic cavity based AMMs. Engine exhaust systems, gas or fluid transmission lines, ventilation systems including pipes provide a guide for the noise propagation caused by the noise source such as engine, fan etc. Therefore, they transmit sound from the source to the environment through the ducts. Works on these kinds of problems go beyond 1920's (Munjal, 1987). Expansion Chambers (ECs) and Helmholtz Resonators (HRs) are very basic acoustic units which are widely used in muffler design with their different forms and combinations (Munjal, 1987) and preferred as unit cells of AMMs as well. Since they are easy to design, cheaper to produce, their theories are explicit and they can present higher transmission losses, they are attracted much by the researchers in the design and analyses of AMMs (Alonso-Redondo et al., 2015; Brillouin, 2003; Croënne et al., 2011; Gebrekidan, Kim, & Song, 2019; Jiménez, Cox, Romero-García, & Groby, 2017; Jung, Kim, & Lee, 2018; Kaina, Fink, & Lerosey, 2013; Lan, Li, Yu, Li, & Liu, 2017; Sharma & Sun, 2015; Theocharis, Richoux, García, Merkel, & Tournat, 2014; Wang & Mak, 2012; Yamamoto, 2018).

The literature summary on other specific issues such as visco-thermal losses and band gap behaviour of acoustic metamaterials are outlined under individual subjects in Chapter 3 for well understanding and consistency with the thesis structure.

1.3 Thesis Organization

The thesis starts with an Introduction section including motivation and objective of the thesis in Chapter 1.

Chapter 2 presents theoretical background of sound wave propagation with acoustic performance parameters, transfer matrix method and effective medium theory.

Chapter 3 includes the design and numerical evaluations of acoustic transmission line metamaterials.

Chapter 4 presents design, numerical and experimental analyses of several cavity based-panel type acoustic metamaterials.

Finally, the thesis ends with a Conclusion section involving further studies.

CHAPTER TWO

THEORETICAL BACKGROUND

2.1 Wave Propagation in 1D medium

A homogenous wave equation in a 1D medium can be given as (Fahy, 2003)

$$\frac{\partial^2 p(x,t)}{\partial x^2} - \frac{1}{c^2}\frac{\partial^2 p(x,t)}{\partial t^2} = 0\,, \tag{2.1}$$

where $p(x,t)$ is the sound pressure propagating in the direction of *x*, $c = \sqrt{B/\rho_0} = \sqrt{1/C\rho_0}$ is the speed of sound (*B* is the Bulk modulus of air, *C* is the compressibility (inverse of *B*), ρ_0 is the mass density of air). The time-harmonic general solution of Eq. (2.1) can be of the following form:

$$p = \left(Ie^{jkx} + Re^{-jkx}\right)e^{-j\omega t}\,. \tag{2.2}$$

Here *I* and *R* are the magnitudes of right- and left-going waves, respectively. $k = \omega / c$ is the complex wavenumber, ω is the circular frequency of the propagating wave and $j = \sqrt{-1}$. Now, consider a propagating plane wave associated with a boundary at *x*=0, as shown in Fig. 2.1, the total wave field $p_{tot,1}$ and $p_{tot,2}$ for medium 1 and 2, respectively, can be written in terms of incident p_i, reflected p_r and transmitted p_t waves as

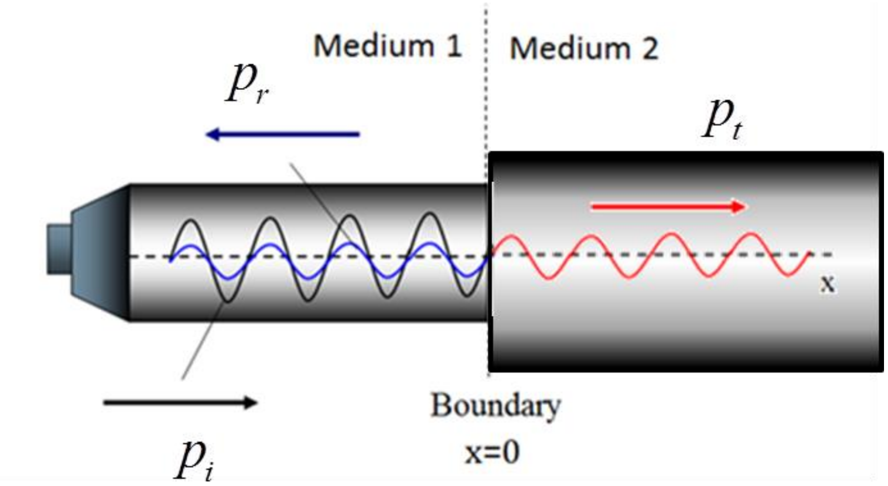

Figure 2.1 Pressure wave field in 1D medium

$$p_{tot,1} = p_i + p_r = Ie^{j(\omega_1 t - k_1 x)} + Re^{j(\omega_1 t + k_1 x)} \ , \tag{2.3}$$

$$p_{tot,2} = p_t = Te^{j(\omega_1 t - k_2 x)} \ . \tag{2.4}$$

An expression for the total particle velocity field $u_{tot,n}$ (n=1, 2) can be derived by using linearized momentum equation for an inviscid perfect gas as follows (Fahy, 2003)

$$\rho_0 \frac{\partial u_{tot,n}}{\partial t} = -\frac{\partial p_{tot,n}}{\partial x} \ . \tag{2.5}$$

Solving Eq. (2.5) by integrating the pressure expression yields

$$u_{tot,n} = -\frac{1}{\rho_0} \int \frac{\partial p_{tot,n}}{\partial x} dt \ . \tag{2.6}$$

Writing Eq. (2.6) explicitly for the medium 1 and 2 yields that, with noting $k_1 = k_2 = k$ and specific air impedance $Z_0 = \rho_0 c$,

$$u_{tot,1} = \frac{1}{Z_0}\left(p_i - p_r\right) \;, \tag{2.7}$$

$$u_{tot,2} = \frac{1}{Z_0} p_t \;. \tag{2.8}$$

Acoustic impedance at a position x can then be found by dividing total pressure by total velocity field;

$$Z\left(x\right) = Z_0 \frac{\left(p_i + p_r\right)}{\left(p_i - p_r\right)} = Z_0 \frac{Ie^{-jkx} + Re^{jkx}}{Ie^{-jkx} - Re^{jkx}} \;. \tag{2.9}$$

At a boundary x=0

$$Z\left(0\right) = Z_0 \frac{I+R}{I-R} \;. \tag{2.10}$$

Reflection, transmission and absorption coefficients can also be derived at x=0;

$$r = \frac{R}{I} \;, \tag{2.11}$$

$$t = \frac{T}{I} \;, \tag{2.12}$$

$$\alpha = 1 - r^2 - t^2 \;, \tag{2.13}$$

respectively. For measuring acoustic impedance of a material by using a standard standing wave impedance tube system, it is suitable to rewrite the impedance expression in Eq. (2.9) with a phase shift. By this way, the equation at impedance end, say $x = L$, can be rewritten as

$$Z\left(L\right)=Z_0\frac{1+re^{j\theta}}{1-re^{j\theta}}, \tag{2.14}$$

where θ is the phase shift and can be defined for a standing wave in a duct as

$$\theta = 2k(L-x)-(2n-1)\pi . \tag{2.15}$$

Note that $(L-x)$ here the distance from the impedance end to the first minimum pressure in the pressure field (n=1).

2.2 Transfer Matrix Method (TMM)

Transfer matrix method (TMM) is a one dimensional analytical method for the determination of acoustic performance parameters. It is widely used in design and analysis of mufflers for acoustic transmission lines. The transfer matrix relates the pressure p_i and particle velocity u_i at the inlet and outlet boundaries of an acoustic unit as shown in Fig. 2.2.

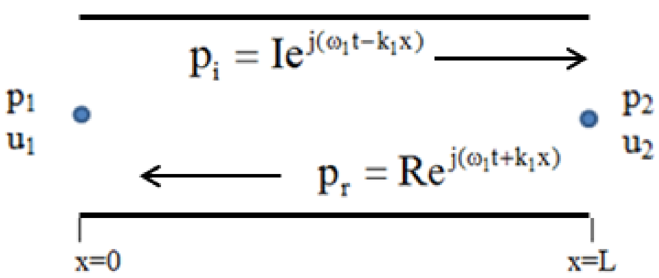

Figure 2.2 A uniform pipe unit

Sound pressure field in a pipe filled with a fluid has a refraction index n can be written for any frequency ω,

$$p_{\text{pipe}}\left(x\right)=I\mathrm{e}^{-jknx}+R\mathrm{e}^{jknx}. \tag{2.16}$$

For air $n=n_0=1$ and $k=k_0$, Equation (2.16) can be written in terms of real and imaginary parts as follows

$$p_{\text{pipe}}(x) = (I+R)\cos k_0 x - j(I\text{-}R)\sin k_0 x\,. \tag{2.17}$$

Particle velocity field in the pipe unit can also be written as

$$u_{\text{pipe}}(x) = \frac{(\text{I-}R)}{Z_0}\cos k_0 x - j\frac{(\text{I+}R)}{Z_0}\sin k_0 x\,. \tag{2.18}$$

Using Eqs. (2.17) and (2.18), following port parameters are found:
i) At boundary x=0

$$p_1 = p_{\text{pipe}}(0) = I + R\,, \tag{2.19}$$

$$u_1 = u_{\text{pipe}}(0) = \frac{I\text{-}R}{Z_0}\,. \tag{2.20}$$

ii) At boundary x=L

$$p_2 = p_{\text{pipe}}(L) = (I+R)\cos k_0 L - j(I\text{-}R)\sin k_0 L\,, \tag{2.21}$$

$$u_2 = u_{\text{pipe}}(L) = \frac{(I\text{-}R)}{Z_0}\cos k_0 L - j\frac{(I+R)}{Z_0}\sin k_0 L\,. \tag{2.22}$$

Rewriting Eqs. (2.21) and (2.22) using Eqs. (2.19) and (2.20) yields that

$$p_2 = p_1\cos k_0 L - u_1 jZ_0\sin k_0 L\,, \tag{2.23}$$

$$u_2 = u_1 \cos k_0 L - p_1 \frac{j}{Z_0} \sin k_0 L \quad . \tag{2.24}$$

These port equations can be written in a matrix form as

$$\begin{Bmatrix} p_2 \\ u_2 \end{Bmatrix} = \begin{bmatrix} \cos k_0 L & -jZ_0 \sin k_0 L \\ -j/Z_0 \sin k_0 L & \cos k_0 L \end{bmatrix} \begin{Bmatrix} p_1 \\ u_1 \end{Bmatrix}, \tag{2.25}$$

and finally rewriting this matrix in an inverse form yields transfer matrix equation

$$\begin{Bmatrix} p_1 \\ u_1 \end{Bmatrix} = \begin{bmatrix} \cos k_0 L & jZ_0 \sin k_0 L \\ j/Z_0 \sin k_0 L & \cos k_0 L \end{bmatrix} \begin{Bmatrix} p_2 \\ u_2 \end{Bmatrix}. \tag{2.26}$$

Then a transfer matrix of a pipe unit is found as

$$\begin{bmatrix} T_{11} & T_{12} \\ T_{21} & T_{22} \end{bmatrix} = \begin{bmatrix} \cos k_0 L & jZ_0 \sin k_0 L \\ j/Z_0 \sin k_0 L & \cos k_0 L \end{bmatrix}. \tag{2.27}$$

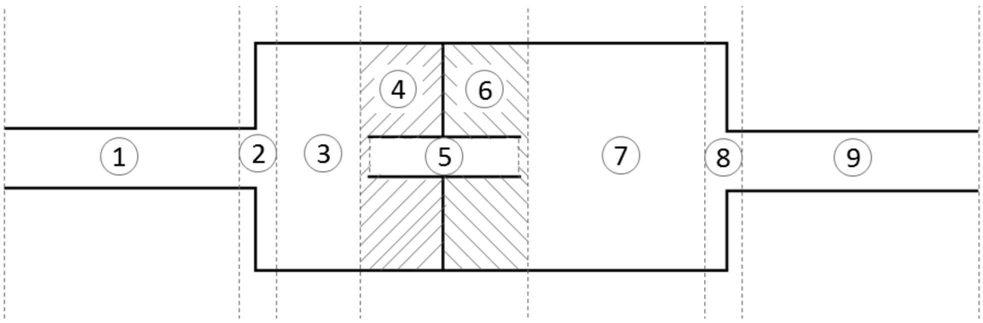

Figure 2.3 Representation of a complex acoustic unit with discontinuity segments

Total transfer matrix of a complex acoustic unit shown in Fig 2.3 can be found by the multiplication of transfer matrix of each individual segment as given below;

$$T^{(s)} = T^{(1)} \times T^{(2)} \times T^{(3)} \times \ldots \times T^{(9)} \quad . \tag{2.28}$$

In order to generalize the transfer matrix, any homogenous medium with effective parameters can be written by modifying the transfer matrix of the pipe section as

$$\begin{bmatrix} T_{e,11} & T_{e,12} \\ T_{e,21} & T_{e,22} \end{bmatrix} = \begin{bmatrix} \cos k_0 n_{eff} L_{eff} & jZ_{eff} \sin k_0 n_{eff} L_{eff} \\ j/Z_{eff} \sin k_0 n_{eff} L_{eff} & \cos k_0 n_{eff} L_{eff} \end{bmatrix} . \quad (2.29)$$

Here L_{eff} is the effective length of the homogenous medium.

2.3 Acoustic Metamaterials (AMMs)

Acoustic metamaterials (AMMs) are generally defined as the material exhibiting extraordinary material behaviour beyond the physical properties of conventional isolation materials, such as negative effective mass density and effective Bulk modulus (inverse of compressibility). Negative effective compressibility is observed in cavity type resonator units whereas negative effective mass density is obtained in structural resonators such as membrane and spring-mass type resonators as shown in Fig. 2.4a and b respectively. Here in this section, one can find resonance frequencies and transfer matrix of several AMM units.

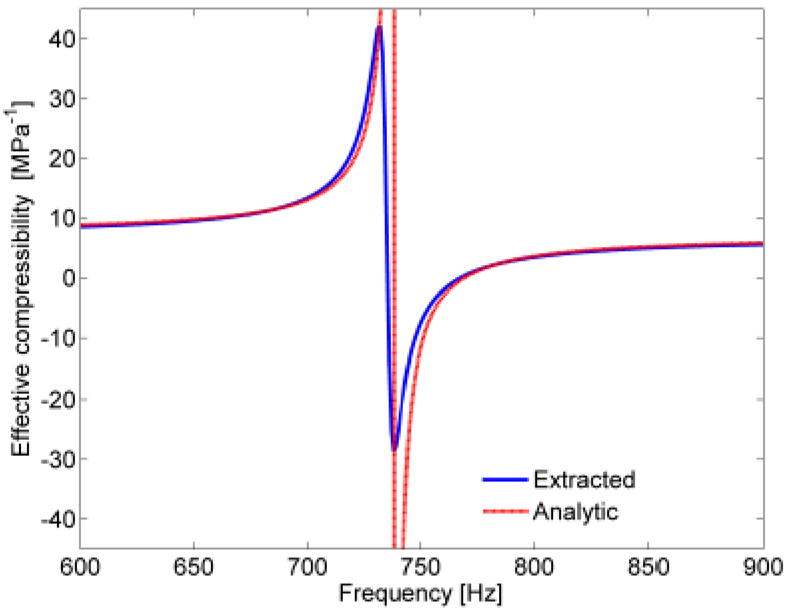

a)

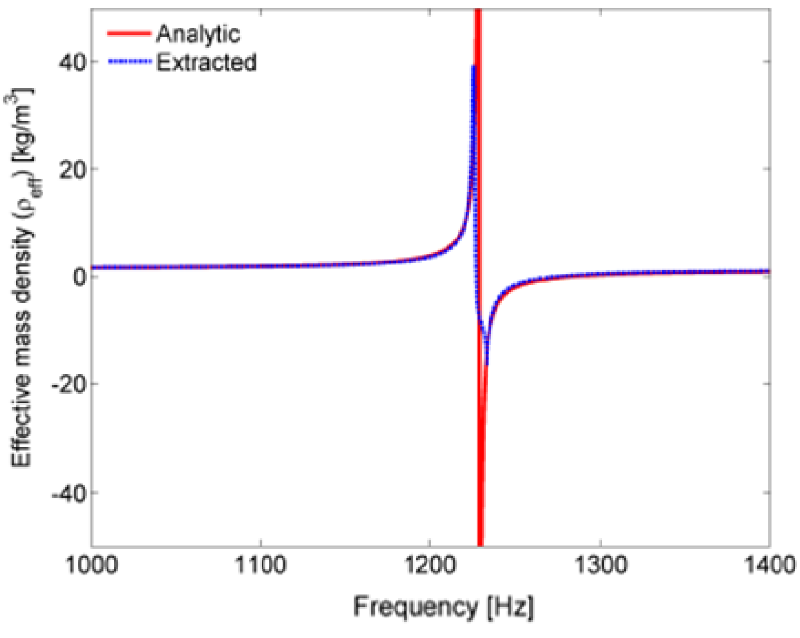

b)

Figure 2.4 a) Negative effective Bulk Modulus of Helmholtz resonator b) Negative effective mass density of a vibrating membrane (Cselyuszka, 2015)

2.3.1 Resonant Metacell Units

Here in this section, resonance frequencies of several different types of metacell units are given. The transfer matrix (TM) of these units is also presented in this section.

2.3.1.1 Cavity Resonator Units

Several cavity resonators; Helmholtz resonators (HR), Half-wavelength resonator (HWR), Quarter-wavelength resonator (QWR) and In-Line Spherical Cavity (ILSC) are schematically shown in Fig 2.5. Helmholtz resonator (HR) is the most attracted one by the designers because it is very handy to manipulate the sound wave by proper selection of neck length, area and cavity volume.

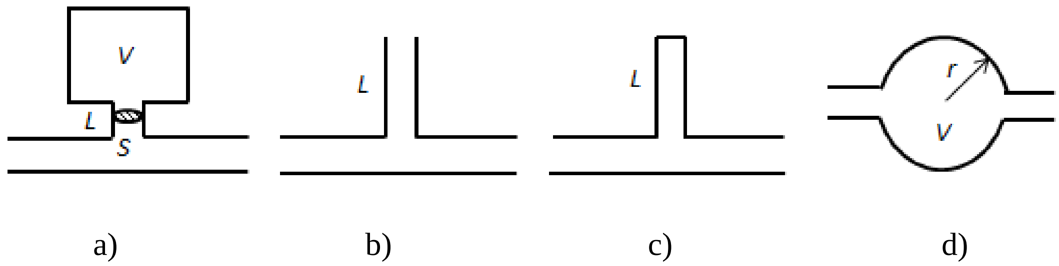

Figure 2.5 a) Helmholtz resonators (HR), b) Half-wavelength resonator (HWR), c) Quarter-wavelength resonator (QWR), d) In-Line Spherical Cavity (ILSC)

The resonance frequency of HR, HWR, QWR and ILSC are given as follows (Mechel, 2008)

$$f_{HR} = \frac{c}{2\pi}\sqrt{\frac{S}{VL'}}, \qquad L' = L + t_w + 0.85 r_n \left(2 - r_n / r_u\right), \tag{2.30}$$

$$f_{HWR} = \frac{c}{2L}, \tag{2.31}$$

$$f_{QWR} = \frac{c}{4L}, \tag{2.32}$$

$$f_{ILSC} = \frac{c}{2\pi r}, \tag{2.33}$$

respectively. The TM of those resonators can be derived as (Mechel, 2008)

$$T = \begin{bmatrix} 1 & 0 \\ 1/Z & 1 \end{bmatrix}. \tag{2.34}$$

Acoustic impedances of these resonators Z in Eq. (2.34) can be written for each resonator type as follows (Mechel, 2008);

$$Z = Z_{HR} = \rho_0 \frac{\omega^2}{\pi c}\left(2 - \frac{r_n}{r_u}\right) + j\rho_0\left(\frac{\omega L'}{S} - \frac{c^2}{\omega V}\right), \tag{2.35}$$

$$Z = Z_{HWR} = j\rho_0 c \tan(k_0 L), \tag{2.36}$$

$$Z = Z_{QWR} = -j\rho_0 c \cot(k_0 L), \tag{2.37}$$

$$Z = Z_{ILSC} = \frac{\rho_0 c^2}{j\omega V}. \tag{2.38}$$

In the above formulas, S is the cross-sectional area of the HR's neck, V is the cavity volume, L' is the effective length of the resonator neck. r_u is the radius of the duct, r_n, L and t_w are the radius, length and the thickness of the HR's neck, respectively.

2.3.1.2 Structural Resonator Units

Structural resonator units can be of membrane form (continuous) or spring-mass-dashpot (lumped) form. Regardless of their forms, their TM can be found in terms of mechanical impedance Z_m as follows (Mechel, 2008)

$$T = \begin{bmatrix} 1 & Z_m \\ 0 & 1 \end{bmatrix} \tag{2.39}$$

The mechanical impedance can be given by means of equivalent mass M_{eq}, stiffness K_{eq} and damping constants C_{eq}.

$$Z_m = j\omega M_{eq} + C_{eq} + \frac{K_{eq}}{j\omega} \tag{2.40}$$

As it is well known that resonance frequency of structural units can be computed by

$$f_R = \frac{1}{2\pi}\sqrt{\frac{K_{eq}}{M_{eq}}}\left(1 - \frac{C_{eq}^2}{2K_{eq}M_{eq}}\right). \tag{2.41}$$

2.3.2 Effective Medium Theory

In this section, the process of retrieving homogenous parameters is outlined based on effective medium theory. Homogenous parameters are effective parameters that characterize a complex acoustic unit in terms of refraction index n_{eff}, acoustic impedance Z_{eff}, mass density ρ_{eff} and compressibility C_{eff}. This is generally carried out by retrieving effective medium parameters using inverse methods, such as the Nicholson-Ross-Weir (NRW) Model (Nicolson & Ross, 1970), scattering parameters modelling (X. Chen, Grzegorczyk, Wu, Pacheco, & Kong, 2004; Szabo, Park, Hedge, & Li, 2010), reflection and transmission coefficients modelling (Fokin, Ambati, Sun, & Zhang, 2007).

Here the inverse approach is applied to the non-homogenous medium by using transfer matrix method. According to this theory, the total transfer matrix of a complex unit, for example the unit shown in Fig. 2.3, can be equalized to effective medium transfer matrix; i.e, equalling Eq. 2.28 to 2.29 yields that;

$$\mathrm{T}^{(s)}=\mathrm{T}^{(1)}\cdot\mathrm{T}^{(2)}\cdot\mathrm{T}^{(3)}\cdot\ldots\cdot\mathrm{T}^{(9)}=\begin{bmatrix}\cos k_0 n_{eff} L_{eff} & jZ_{eff}\sin k_0 n_{eff} L_{eff}\\ j/Z_{eff}\sin k_0 n_{eff} L_{eff} & \cos k_0 n_{eff} L_{eff}\end{bmatrix} \tag{2.42}$$

Then acoustic performance parameters; transmission, reflection and absorption coefficients can be derived using Eq. (2.42) as follows

$$t=\frac{2}{T_{\mathrm{e},11}+\dfrac{T_{\mathrm{e},12}}{Z_0}+Z_0T_{\mathrm{e},21}+T_{\mathrm{e},22}}, \tag{2.43}$$

$$r=\frac{T_{\mathrm{e},11}+\dfrac{T_{\mathrm{e},12}}{Z_0}-Z_0T_{\mathrm{e},21}-T_{\mathrm{e},22}}{T_{\mathrm{e},11}+\dfrac{T_{\mathrm{e},12}}{Z_0}+Z_0T_{\mathrm{e},21}+T_{\mathrm{e},22}}, \tag{2.44}$$

$$\alpha=1-t^2-r^2. \tag{2.45}$$

By this way, effective medium parameters such as refraction index, acoustic impedance, mass density and compressibility can be retrieved respectively as follows (Seçgin & Baygün, 2019a):

$$n_{eff}=\frac{1}{k_{eff}L_{eff}}\cos^{-1}\left(T_{e,11}\right), \tag{2.46}$$

$$Z_{eff} = Z_0\left(\frac{1-r}{1+r}\right) \quad \left[\frac{\text{kg}}{\text{m}^2\text{s}}\right], \tag{2.47}$$

$$\rho_{eff} = \frac{n_{eff}}{c} Z_{eff} \quad \left[\frac{\text{kg}}{\text{m}^3}\right], \tag{2.48}$$

$$C_{eff} = \frac{n_{eff}}{cZ_{eff}} \quad \left[\frac{1}{\text{MPa}}\right]. \tag{2.49}$$

For passive medium assumption, the conditions $\text{imag}(n_{eff}) \geq 0$ and $\text{real}(Z_{eff}) \geq 0$ must be satisfied for physical consistency. Retrieval of the real part of refraction index, a mathematical branch problem occurs, since no unique solution exist for the real part due to cosine function. In this respect, effective refraction index must be rewritten in the form as (Szabo et al., 2010);

$$n_{eff}(\text{m},\omega) = \frac{1}{k_{eff}l_{eff}}\left(\text{real}\left(\cos^{-1}\left(T_{11}\right)\right) + 2\pi\text{m}\right) + \frac{\text{j}}{k_{eff}l_{eff}}\text{imag}\left(\cos^{-1}\left(T_{11}\right)\right) \; . \tag{2.50}$$

Here m is the branch number and can be predicted by Kramers-Kronig refraction index (Szabo et al., 2010):

$$\text{m}_i = \text{round}\left[\left(n_{K-K}(\omega_i) - \text{real}(n_{eff}(0,\omega_i))\right)\right]. \tag{2.51}$$

Here, i is the index of frequency vector ω, $n_{K-K}(\omega(i))$ is Kramer-Kronig refraction index at ith frequency, which can be given as (Szabo et al., 2010)

$$n_{K-K}(\omega_i) = 1 + \frac{2}{\pi}\wp\left(\int_0^\infty \frac{\omega_{i+1}\cdot\text{imag}\left(n_{eff}(0,\omega_{i+1})\right)}{\omega_{i+1}^2 - \omega_i}d\omega\right), \tag{2.52}$$

where $\wp$ denotes principal value of the integral.

2.3.3 Analytical Visco-Thermal Models

For a realistic acoustic model of an acoustic transmission line, acoustic performance parameters such as sound transmission, reflection and absorption coefficients should be predicted by including visco-thermal (v-t) effects. It is shown that those effects influence slow sound propagation in systems with side resonators (Theocharis et al., 2014). Moleron et al. (2015) experimentally investigated visco-thermal effects for the metamaterials composed of rigid slabs and demonstrated that visco-thermal effects should not be avoided for actual acoustic response. These effects are generally treated in the models by two manners; analytical and numerical. The theories of them are based on full set of Navier-Stokes (N-S) equations. Tijdeman (1975) states that approximate analytical models for circular ducts are generally grouped in two divisions. The first group formulates these effects based on Kirchhoff solutions to complex transcendental equations. The second group uses more basic governing equations known as Low Reduced Frequency (LRF) solution. Zwikker-Kosten model (Zwikker & Kosten, 1949) is one of the well-known models of this kind, and it is commonly used in acoustics to include the visco-thermal losses (Seçgin & Baygün, 2019a; Theocharis et al., 2014). The assumption in LRF is that the propagation wavelength is large compared with a characteristic length of the problem and boundary layer thickness. Finite element method is very flexible numerical tool to handle v-t effect. In FE computations, two methodologies are used based on the selection of field variables i) 2 field variables: temperature variation, particle velocities (Beltman, 1998) ii) 3 field variables: temperature variation, particle velocities and sound pressure (Joly, 2008; Kampinga, Wijnant, & de Boer, 2010; Malinen, Lyly, Råback, Kärkkäinen, & Kärkkäinen, 2004). Cordioli et al. (2010) showed that the latter presents more accurate results when compared with experiments, since it is capable of dissipation due to discontinuities.

As it is mentioned above, two groups of analytical methods are generally applied for visco-thermal effects for circular tubes. The first group is based on Kirchhoff solution (KS) model and the second one is low reduced frequency (LRF) model. A comprehensive discussion on this issue can be found in Ref. (Tijdeman, 1975). Here two models from these two groups are briefly discussed; a KS model of Kirchhoff (Tijdeman, 1975) and a LRF model of Zwikker-Kosten (Zwikker & Kosten, 1949). Here the connection between several methods belong to both groups are also given.

2.3.3.1 Kirchhoff Solution (KS) Visco-thermal Model

For “wide” circular tubes ($R >> d_{visc}$), modifying Kirchhoff formulas (Tijdeman, 1975), one can end up with the following wavenumbers corresponding to viscos and thermal losses;

$$k_{visc} = \frac{(1-\mathrm{j})}{R\sqrt{2}} d_{visc} , \tag{2.53}$$

$$k_{therm} = \frac{(1-\mathrm{j})}{R\sqrt{2}} (\gamma - 1) d_{therm} , \tag{2.54}$$

respectively. Here R is the radius of the circular duct and γ is heat capacity ratio and d_{visc} and d_{therm} are thicknesses of viscos and thermal boundary layers, respectively and can be written as (Tijdeman, 1975)

$$d_{visc} = \sqrt{\frac{2\mu}{\rho_0 \omega}} , \tag{2.55}$$

$$d_{therm} = \frac{d_{visc}}{\sqrt{\mathrm{Pr}}} , \tag{2.56}$$

respectively. Here μ is the dynamic viscosity, Pr is the Prandtl number for air medium. Defining shear wavenumber (also known as Stoke’s number) as $s = R / d_{visc}$ for “very wide” tubes, $\lim_{s\to\infty} k = k_0$ being the solution of plane wave in the absence of viscos and thermal effects. For small values of shear wavenumber, Kirchhoff formula reduces to Rayleigh solution:

$$k \approx 2(1-\mathrm{j})\frac{\sqrt{\gamma}}{R}d_{visc}\,. \tag{2.57}$$

2.3.3.2 Low Reduced Frequency (LRF) Visco-thermal Model

In this v-t model, the first assumption is that the internal tube radius is small in comparision with the wavelength of propagation, this states that the reduced frequency i.e., $k_r = k_0 R << 1$. The second assumption is that the radial velocity component, v is small with respect to the axial velocity, i.e., $v/u << 1$ (Tijdeman, 1975). One of the well-known for this kind of models is Zwicker-Kosten model. The reduced wavenumber is defined in terms of zeroth and second order of the first kind of Bessel function (Zwikker & Kosten, 1949):

$$k_r = -j\sqrt{\frac{\mathrm{J}_0\left\langle \mathrm{i}^{3/2}s\right\rangle}{\mathrm{J}_2\left\langle \mathrm{i}^{3/2}s\right\rangle}}\sqrt{\gamma/\sigma}\,, \tag{2.58}$$

where σ is determined as

$$\sigma = \left[1+\left(\frac{\gamma-1}{\gamma}\right)\frac{\mathrm{J}_2\left\langle \mathrm{i}^{3/2}s\sqrt{\mathrm{Pr}}\right\rangle}{\mathrm{J}_0\left\langle \mathrm{i}^{3/2}s\sqrt{\mathrm{Pr}}\right\rangle}\right]^{-1}. \tag{2.59}$$

When $\sigma = \gamma$, Eq. (2.58) reduces to Kerris v-t approximation. Tijdeman (1975) shows that the Zwikker-Kosten model covers the solutions of other form of LRF models. The model has also been validated by Stinson (1991) for circular tubes complying with the conditions of $R > 10^{-3}\mathrm{cm}$ and of $R(\omega/c_0)^{3/2} < 10^{6}\mathrm{cms}^{-3/2}$.

2.3.3.3 Band Gap Behaviour

It is known that AMMs may create three different band gaps where the transmissions of waves are inhibited. These band gaps can be classified as (Lu et al., 2013) i) Bragg Gap (BG), ii) Hybridization Gap (HG), iii) Local Resonant Gap (LRG). As it is previously pointed out that the BGs typically occur in Phononic Crystals (PCs) due to the destructive interference of waves scattered from periodic inhomogeneities at wavelengths of propagation. In BGs, the wavelength of the propagation is comparable to the spatial periodicity of the lattice (Brillouin, 2003; Kaina et al., 2013). Therefore the gap is strongly dependent on the lattice constant stating cellular periodicity and thus it is generally observed in higher frequencies since PCs have generally small lattice constants. The centre frequency of this gap is defined as (Lu et al., 2013)

$$f_{BG} \approx c / 2a \quad , \tag{2.60}$$

where c is the propagation speed of wave in the medium, a is the lattice constant. Although this band gap occurs in PCs, it can also be observed in acoustic metamaterials having periodic unit cells. HGs occur due to the coupling between scattering resonances of the individual material unit and the propagating mode of the embedding medium, with a centre frequency (Lu et al., 2013);

$$f_{HG} \approx c_p / 2L \quad , \tag{2.61}$$

where c_p is the propagation speed characterizing the resonance mode, L is the characteristic length of the material unit. The third type is due to local resonance of the material unit in a form of cavity or structural element. This gap generally exhibit narrow band character and occurs at individual resonance frequency of unit cells. All these gaps can be adjusted by spatial periodicity and physical constitute of cells composing the metamaterial. The spatial periodicity of unit cells also creates periodic boundaries leading to full (in lossless case) transmission at certain frequencies known as Fabry-Perot (FP) frequencies. (m-1) number of FPs approximately occurs at (Moleron et al., 2015)

$$f_{FP} = mc / 2n_{eff} L_{eff}\,,\; m = 1, 2, \cdots \tag{2.62}$$

where m is an integer showing number of periodic boundaries, L_{eff} is the effective length of the metamaterial, not the lattice constant. For lossy case, absorption is enhanced at these F-P frequencies, since no reflection due to full transmission (Note that the transmission will not be full due to visco-thermal effects at all). Therefore the periodicity or cellular arrangement of a metamaterial influences not only frequency band characteristics but also acoustic performance parameters.

CHAPTER THREE
DESIGN OF ACOUSTIC TRANSMISSION LINE METAMATERIALS

3.1 In Line Spherical Cavity (ILSC)-type Metamaterial with and without Visco-Thermal Effect

This section of the chapter concerns with defining effective medium parameters- such as refraction index, impedance, mass density and compressibility- of acoustic metamaterials via an inverse method based on transfer matrix method (TMM) with and without taking of v-t effect into account. The formulations and background theory are given in Chapter 2. Here, v-t effects are approximately defined in the transfer matrix equations by using Kirschoff model. Acoustic parameters such as transmission and absorption coefficients are also computed via TMM.

In the study, as an example, an in-line spherical cavity (ILSC) based acoustic metamaterial is considered. The effect of v-t losses on acoustic parameters and effective parameters is discussed for the considered acoustic metamaterial. It is shown that v-t effects cannot be avoided for numerical designs leading to practical predictions.

3.1.1 Total Transfer Matrix of the ILSC-type Metamaterial

In this section, homogenization of an in-line spherical cavity (ILSC) based metamaterial consist of three metacells are carried out by using inverse method based on transfer matrix elements. In this respect, the transfer matrix of the metamaterial shown in Fig 3.1.a can be equalized to the transfer matrix of a passive material shown in Fig 3.1.b. By this way, effective parameters such as refraction index and acoustic impedance can be retrieved from this equalization.

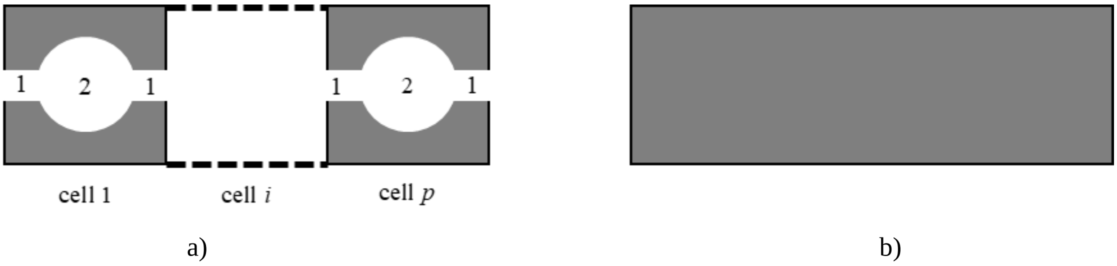

Figure 3.1 a) ILSC metamaterial b) A passive material (Seçgin & Baygün, 2019a)

The total transfer matrix (TM) of the metamaterial shown in Fig. 3.1a can be found by the multiplication of the individual TMs of each acoustic segments (cells); slit (1)-cavity (2)-slit (1). The transfer matrix of the slit (1) and the cavity (2) can be written as:

$$\mathrm{T}_{\mathrm{ILSC}} = \prod_{\mathrm{i=1}}^{\mathrm{p}} \left(\begin{bmatrix} \cos kl_{slit} & jZ\sin kl_{slit} \\ \dfrac{j}{Z}\sin kl_{slit} & \cos kl_{slit} \end{bmatrix} \begin{bmatrix} 1 & 0 \\ \dfrac{jkV_{\mathrm{cavity}}}{\rho_0 c} & 1 \end{bmatrix} \begin{bmatrix} \cos kl_{slit} & jZ\sin kl_{slit} \\ \dfrac{j}{Z}\sin kl_{slit} & \cos kl_{slit} \end{bmatrix} \right)_{\mathrm{i}} \tag{3.1}$$

Here, p is the number of cell, l_{slit} is the length of the slit, V_{cavity} is the volume of the cavity.

3.1.2. Numerical Results

Table 3.1 tabulates the physical and material properties of the considered ILSC type acoustic metamaterial considered in the study. In this section, at first, transmission coefficient of a three-cell metamaterial obtained by TMM are verified with that of computed via FEM. Then TMM results of effective impedance and effective refraction index are questioned whether they reflect passive medium character with and without visco-thermal (v-t) effects. Finally, the homogenization scheme is completed to predict effective density and effective compressibility of the materials with one-, two- and three-cell individually in order to show the effect of v-t losses.

Table 3.1 Physical and material properties of ILSC acoustic metamaterial (Seçgin & Baygün, 2019a)

Properties	Parameter	Value
Slit length	l_{slit}	10e-3 m
Slit radius	r_{slit}	5e-3 m
Cavity radius	r_{cavity}	12.5e-3 m
Mass density	ρ_0	1,2 kg/m^3
Speed of sound	c	343 m/s
Dynamic viscosity	μ	1.78e-5 N.s./m^2
Prandtl number	Pr	0.7491
Heat capacity ratio	γ	1.4028

3.1.2.1 Verification study

In this section, the transmission losses predicted by FEM and TMM are compared for three spherical cavity cells as shown in Figure 3.2. Here v-t effects are taken into account in TMM and FEM analyses. In the 2D axisymmetric model, 1616 quadrilateral, 2804 triangular, 684 edge and 51 vertex elements changing in size of 0.04-7.16 mm were applied by providing that each analysis of wavelength has at least 5 elements. Boundary conditions were applied to the input and output ends according to the plane wave theory and the left end is excited by 1 Pa harmonic sound pressure. Depending on the incoming wave, the average sound pressure level at the end surface of the outlet pipe (right end) is obtained, and the transmission coefficient t is calculated by 10 Hz steps, in a range of 20-4000 Hz for the FEM model without v-t effects. In the computations with v-t effect, the analyses were performed for different frequency steps (from 10 to 50 Hz) along the entire frequency range of interest in order to be efficient in computational cost, but to not miss the information especially at the valley-peak zones at the same time. Thickness of viscos boundary layer d_{visc} changing with frequency is calibrated for 100 Hz as

$$d_{visc} = 0.22\sqrt{100/f} \text{ (mm)} \tag{3.2}$$

The Kirschoff model -used here as v-t model in TMM- which has been validated by Stinson (1991) for circular tubes complying with the conditions of $r > 10^{-3}\text{cm}$ and of $rf^{3/2} < 10^{6}\text{cms}^{-3/2}$. The tube and cavity radii and frequency range of analyses considered in this study ensure given conditions, i.e., the v-t model can be reliably used for this ILCS metamaterial.

The comparison shown in Fig. 3.3 states that TMM is sufficiently accurate although small discrepancies and frequency shifts are observed. Arisen peaks and valleys are due to Fabry-Perot (FP) resonances and their numbers are related to the number of cells by minus 1. As it is clear that FP peaks are affected much by v-t effects, even though slight frequency shifts are observed in that resonance peaks. Therefore FP frequencies with a bandwidth are the frequencies one might improve higher absorption.

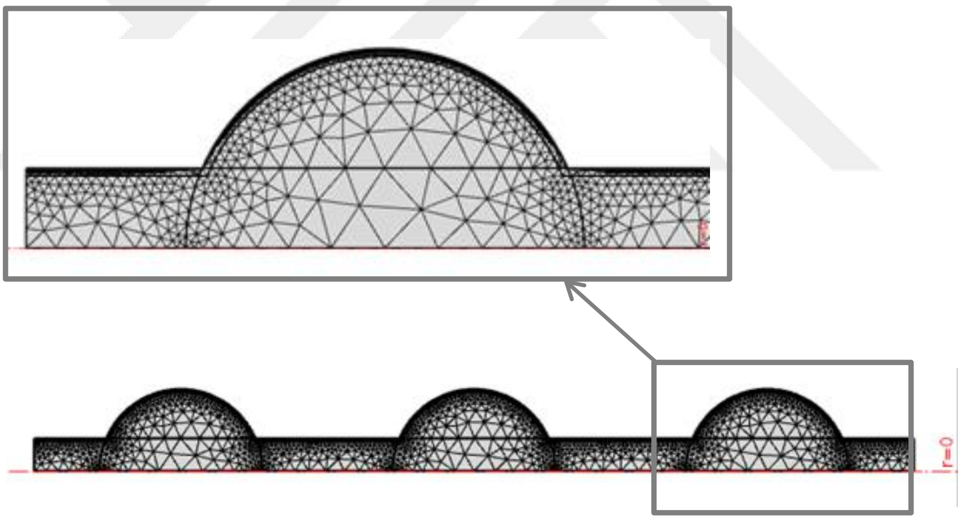

Figure 3.2 2D axisymmetric mesh model of three spherical cavity cells (Seçgin & Baygün, 2019a)

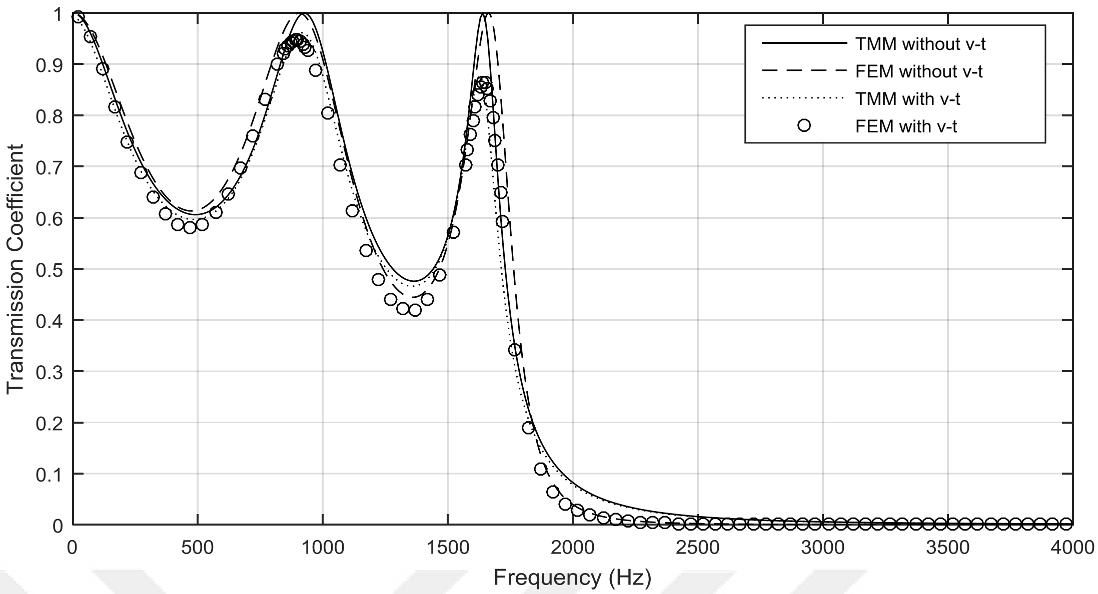

Figure 3.3 Transmission coefficients of three-cell material predicted by TMM and FEM (v-t: visco-thermal losses) (Seçgin & Baygün, 2019a)

3.1.2.2 Retrieving Acoustic and Effective Medium Parameters

Before going through the study for the influence of v-t losses on effective medium parameters, it is valuable to discuss here that the effect of v-t losses on acoustic parameters such as transmission and absorption coefficients which are indicated in Figure 3.4. Note that, here reflection coefficients are not given in the figure for avoiding complexity. The results show that increasing number of cells improves absorption characteristics, especially at Fabry-Perot frequencies appeared as 1340 Hz for two-cell, 940 Hz and 1665 Hz for three-cell in the figure.

Now, effective medium parameters of three-cell material can be determined by applying the homogenization procedure given in Chapter 2. Firstly, it is of importance for realistic determination of effective medium parameters to check whether the homogenization procedure provide passive material characteristics. As it is mentioned in the previous section, this is realized by observing that both imaginary part of effective refractive index and real part of impedance are positive. Fig. 3.5.a and 3.5.b verifies that the homogenization scheme which present positive values for both parameters with and without v-t effects.

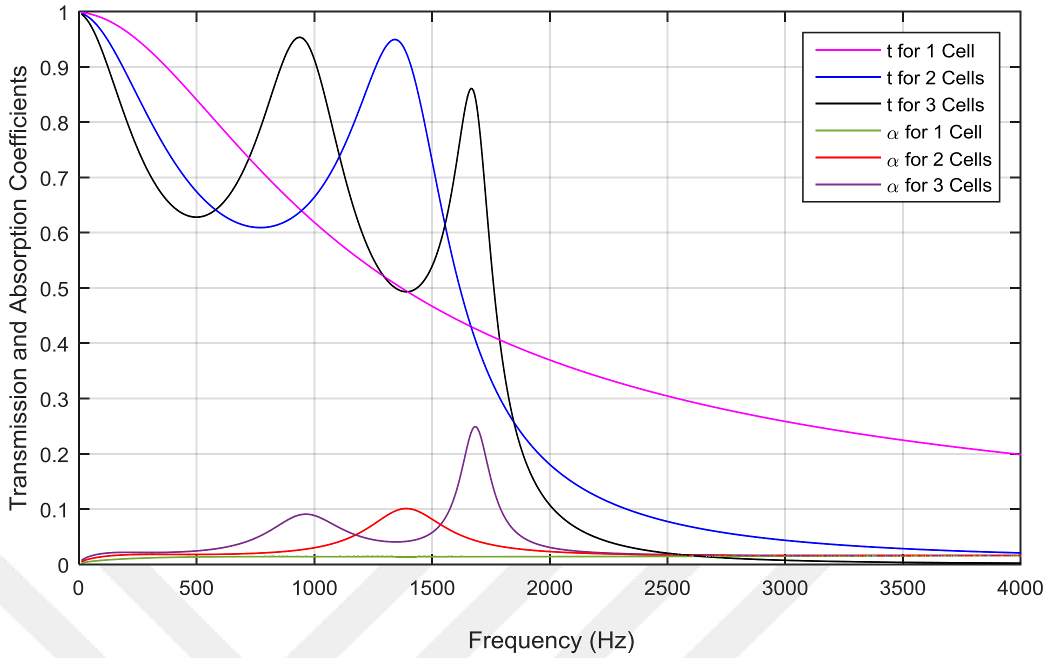

Figure 3.4 Transmission and absorption coefficients of ILSC metamaterials with visco-thermal effects (Seçgin & Baygün, 2019a)

Fig 3.6.a presents the real part of the effective mass density which is always positive. It is seen around 1900 Hz, that a sudden peak occurs where the effective compressibility starts being negative as shown in Figure 3.6.b. At this point, attenuation in the peak due to v-t loss is observed with approximately amount of 50%. In Figure 3.6.b, the effective compressibility becomes negative just after 1900 Hz where the first mode of the spherical cavity occurs. At this resonance frequency the material becomes so-called “meta” since it exhibits negative compressibility behaviour as shown in Figure 3.6b, which results in a stop band behaviour in transmission losses. This behaviour is seen for both the metamaterial with and without loss effects. However, effects of v-t loss are clearly seen as attenuations on the peaks of effective parameters, even though they are not meaningful at stopband region. Therefore it can be said that for the structures having large v-t values can influence the characteristics of the metamaterial, thus it must be taken into account for more realistic designs.

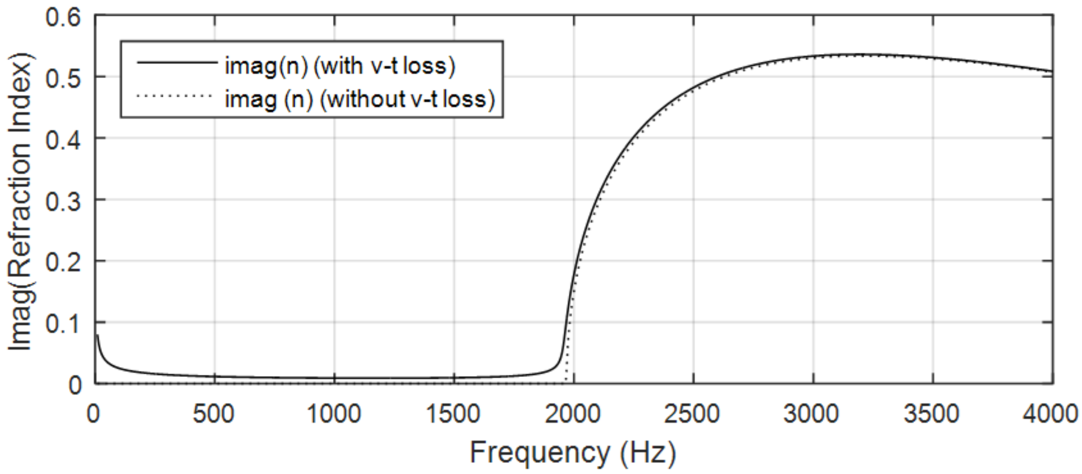

a)

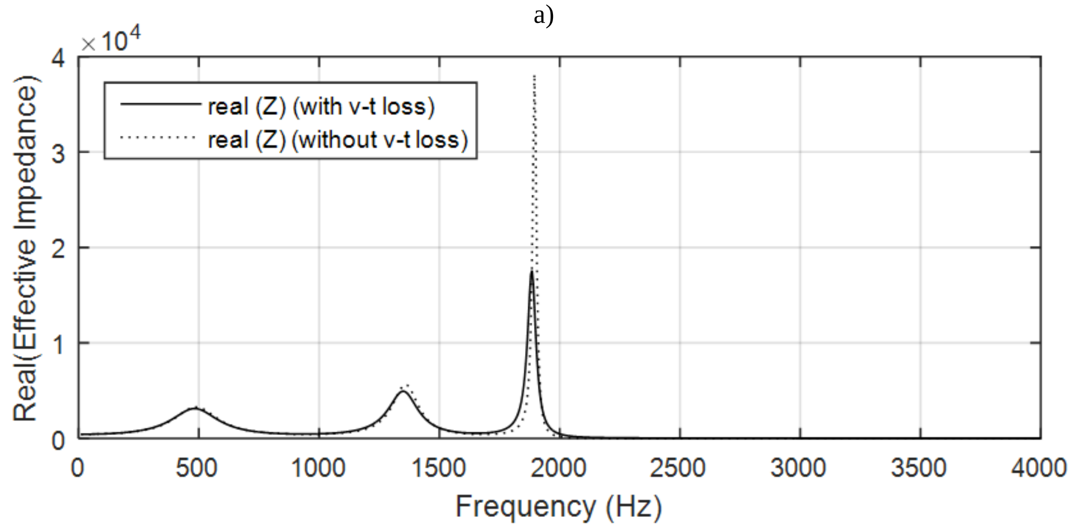

b)

Figure 3.5 a) Imaginary part of effective refractive index, b) real part of effective impedance (v-t loss: visco-thermal losses) (Seçgin & Baygün, 2019a)

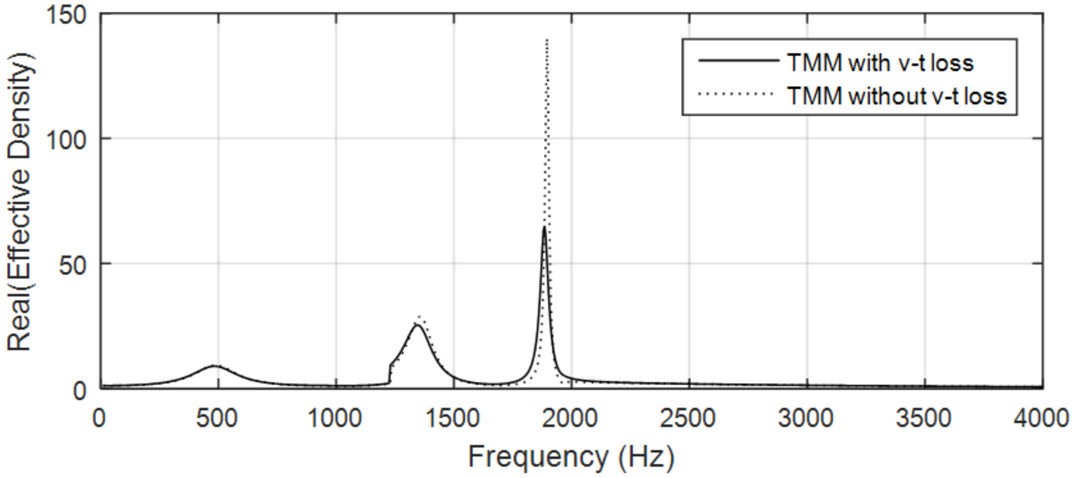

a)

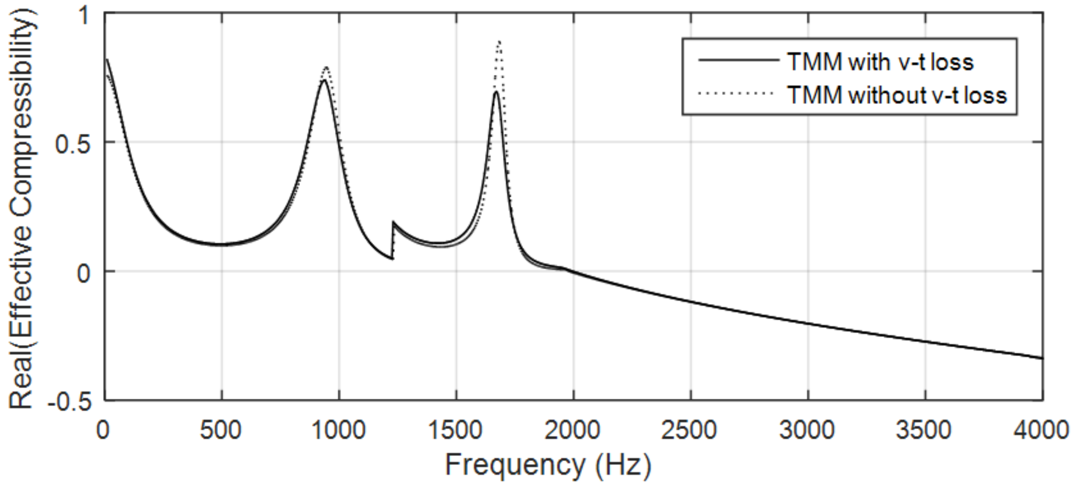

b)

Figure 3.6 a) Real part of effective density, b) real part of effective compressibility (v-t loss: visco-thermal losses) (Seçgin & Baygün, 2019a)

3.2 Expansion Chamber (EC)-type Metamaterial with and without Visco-Thermal Effect

In this part, the effects of cellular periodicity of AMMs composed of several combinations of ECs on acoustic performance parameters are investigated. In this context, three different cellular arrangement with different number of cells regarding on their diameters of expansion are considered (with noting that all have the same acoustic cavity volume in total); i) cells with the same expansion diameters, ii) cells with golden-ratio increasing diameters and iii) cells with linear increasing diameters. It is observed that all material arrangements have single negative properties. The study uses transfer matrix method (TMM) for computational tool by considering visco-thermal effects, and utilizes effective (homogenous) medium parameters in evaluations. During the study, several analytical visco-thermal models are studied and Kirchhoff model is adapted to the transfer matrices. The TMM models with and without visco-thermal effects are verified by Finite Element Method (FEM). Effective parameters of these arrangements are also determined from acoustic performance parameters. The results showed that all three arrangements exhibit single negative material property and different transmission and absorption characteristics.

3.2.1 Total Transfer Matrix of the EC-type Metamaterial

In this section, transfer matrix of an acoustic transmission line metamaterial composed of several number of expansion chamber (EC) type cells are derived. Consider an acoustic transmission line metamaterial shown schematically in Fig 3.7. The two port parameters; sound pressure *p* and particle velocity *u* at ports 1 and *n* can be related by total transfer matrix T_{EC} as;

$$\begin{Bmatrix} p_1 \\ u_1 \end{Bmatrix} = T_{EC} \begin{Bmatrix} p_n \\ u_n \end{Bmatrix} \tag{3.3}$$

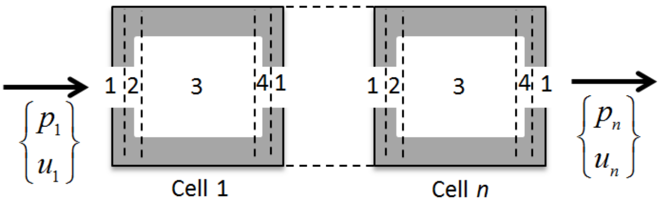

Figure 3.7 An acoustic transmission line metamaterial consists of *n* number of expansion chamber type metacells

The T_{EC} of the metamaterial can be obtained by the multiplication of the individual transfer matrices (TMs) of each acoustic segment; tube (1) - sudden expansion (2) -tube (3) - sudden contraction (4) – tube (1);

$$T_{EC} = \prod_{i=1}^{n} \left(T_1 \cdot T_2 \cdot T_3 \cdot T_4 \cdot T_1 \right)_i \,, \tag{3.4}$$

where *n* is the number of cell in the transmission line. The transfer matrix of tubes 1 and 3 is given by

$$T_{1(3)} = \begin{bmatrix} \cos k_0 n_0 L_{1(3)} & \mathrm{j} Z_0 \sin k_0 n_0 L_{1(3)} \\ \dfrac{\mathrm{j}}{Z_0} \sin k_0 n_0 L_{1(3)} & \cos k_0 n_0 L_{1(3)} \end{bmatrix} \tag{3.5}$$

and, the transfer matrix of sudden expansion and contraction including end corrections for stationary medium is given by (Munjal, 1987);

$$T_{2(4)} = \begin{bmatrix} 1 & \mathrm{j}\omega \left(1 - 1.25 \dfrac{r_1}{r_3} \right) 0.85 \dfrac{r_1}{S_1} \\ 0 & 1 \end{bmatrix}. \tag{3.6}$$

Here, for air medium $n_0 = 1$ is the refraction index of air, r_i and L_i are the radius and length of the *i*.th tube, respectively. S_1 is the cross-section are of the smallest tube (tube 1).

3.2.2 Modelling and Simulations

This section is devoted to present i) firstly a comparison of analytical visco-thermal models, ii) then it includes a verification study of the TMM models by using finite element method, iii) finally, the effects of cellular arrangements of the materials on their acoustic performance are discussed based on the results of TMM simulations. Fig. 3.8 presents the geometrical parameters of EC type materials considered in this analysis.

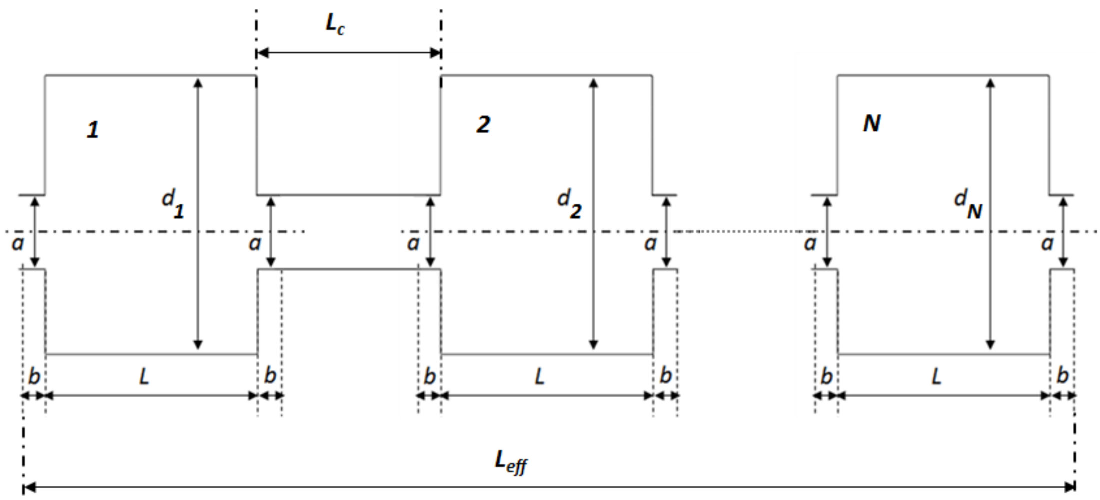

Figure 3.8 Schematic of a metamaterial composed of *N* number of expansion chamber type units

3.2.2.1 Comparision of analytical visco-thermal models

Here, LRF and KS solutions for visco-thermal (v-t) models are compared in Fig. 3.9 for the single EC unit with the following parameters; *a*=10 mm, *L*=50 mm, Pr=0.7491, $\mu = 1.78\times10^{-5}\,\text{Ns/m}^2$, $\rho_0 = 1.2\ \text{kg/m}^3$, $\gamma = 1.4028$. It is seen from the figure that Zwicker –Kosten and Kirchhoff models are quite close to each other, whereas Rayleigh and Kerris models diverge from them. However, all models tend to converge as shear wavenumber goes higher values.

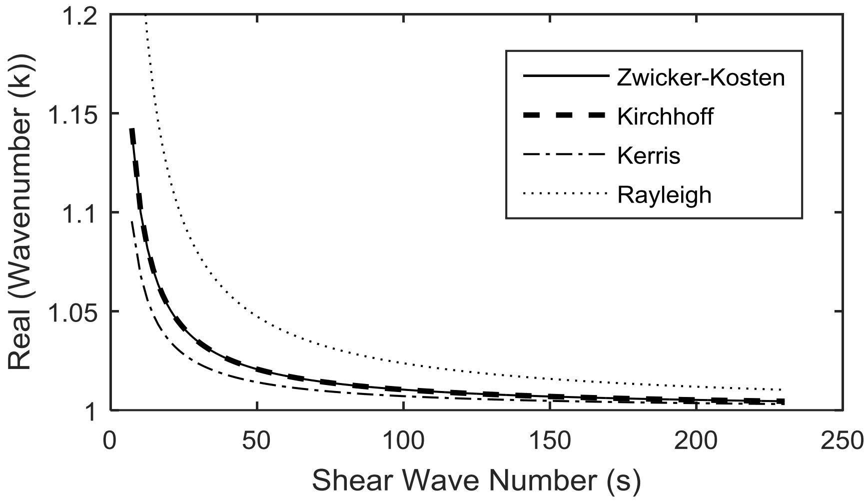

Figure 3.9 Comparision of LRF and KS visco-thermal models

Considering these outcomes, in the next analytical computations, Kirchhoff model will be used in TMM matrices (since it is more straightforward for adaptations) by making following adaptations to wavenumber and to impedance in the transfer matrices of each acoustic segment (Theocharis et al., 2014):

$$k_0 \to k_0\left(1+k_{visc}+k_{therm}\right), \tag{3.7}$$

$$Z_0 \to Z_0\left(1+k_{visc}-k_{therm}\right). \tag{3.8}$$

One can refer to Eqs. 2.53 and 2.54 for the definitions of k_{visc} and k_{therm}, respectively.

3.2.2.2 Verification of TMM using FEM

This section presents the verification of transfer matrix method (TMM) by using finite element method (FEM). Here, two material arrangements are considered;

i) the material with single unit cell (Fig. 3.10),

ii) the material with three-unit cells composed of the same single cells.

Each cell has the following properties; a=12.5 mm, b=5 mm, d=53.904 mm, L=40 mm, Pr=0.7491, $\mu = 1.78\times10^{-5}\,\text{Ns/m}^2$, $\rho_0 = 1.2\ \text{kg/m}^3$, $\gamma = 1.4028$. Comparisons are performed for the cases with and without v-t models. In analytical v-t modelling, KS model is used in TMMs. Since the v-t effects are generally considerable on peaks, FEM v-t computations are carried out only for certain frequency bands covering transmission peaks in order to reduce computational costs and memory usage. Note that the number of finite elements was determined by providing that each analysis of wavelength has at least 5 elements as realized in the previous analysis. Boundary conditions were applied to the input and output ends according to the plane wave theory and the left end is excited by 1 Pa harmonic sound pressure. The $d_{visc} = 0.22\sqrt{100/f}\ \text{(mm)}$ is calibrated for 100 Hz for each frequency of interest.

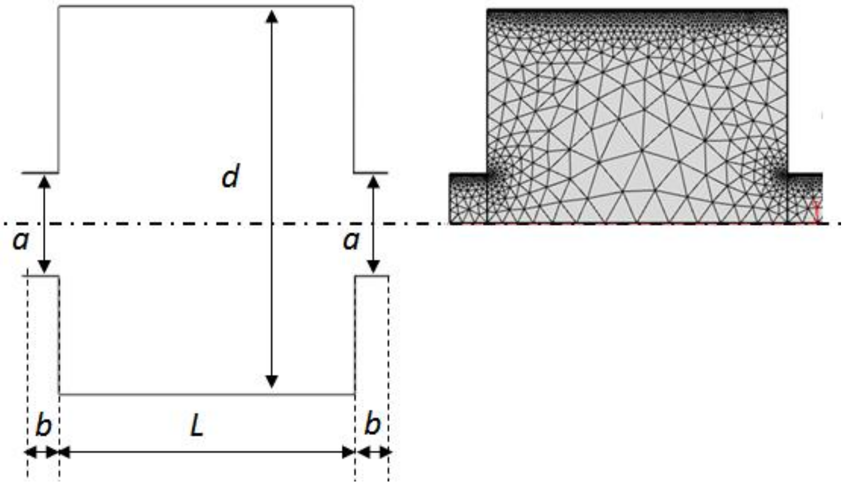

Figure 3.10 Schematic of a single circular expansion chamber type unit and its 2D FE mesh

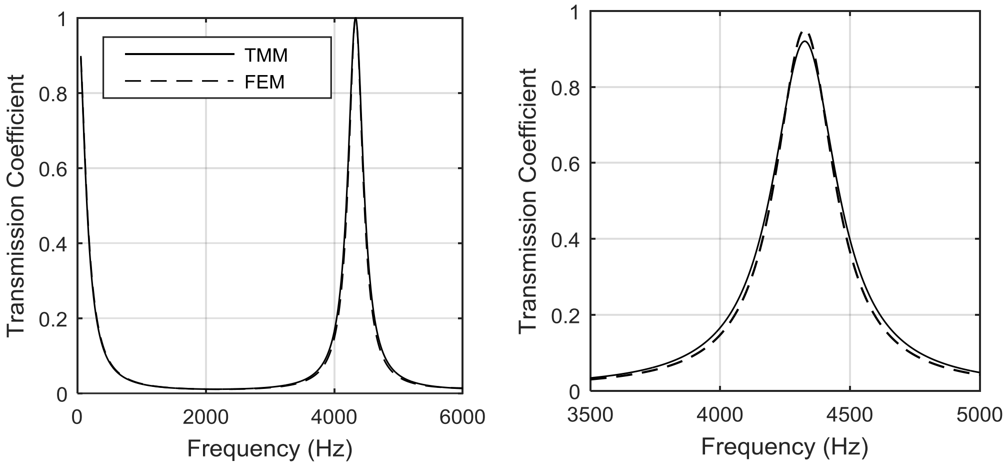

a) b)

Figure 3.11 Verification of TMM by using FEM for the single unit case a) without v-t effects, b) with v-t effects (3500-5000 Hz)

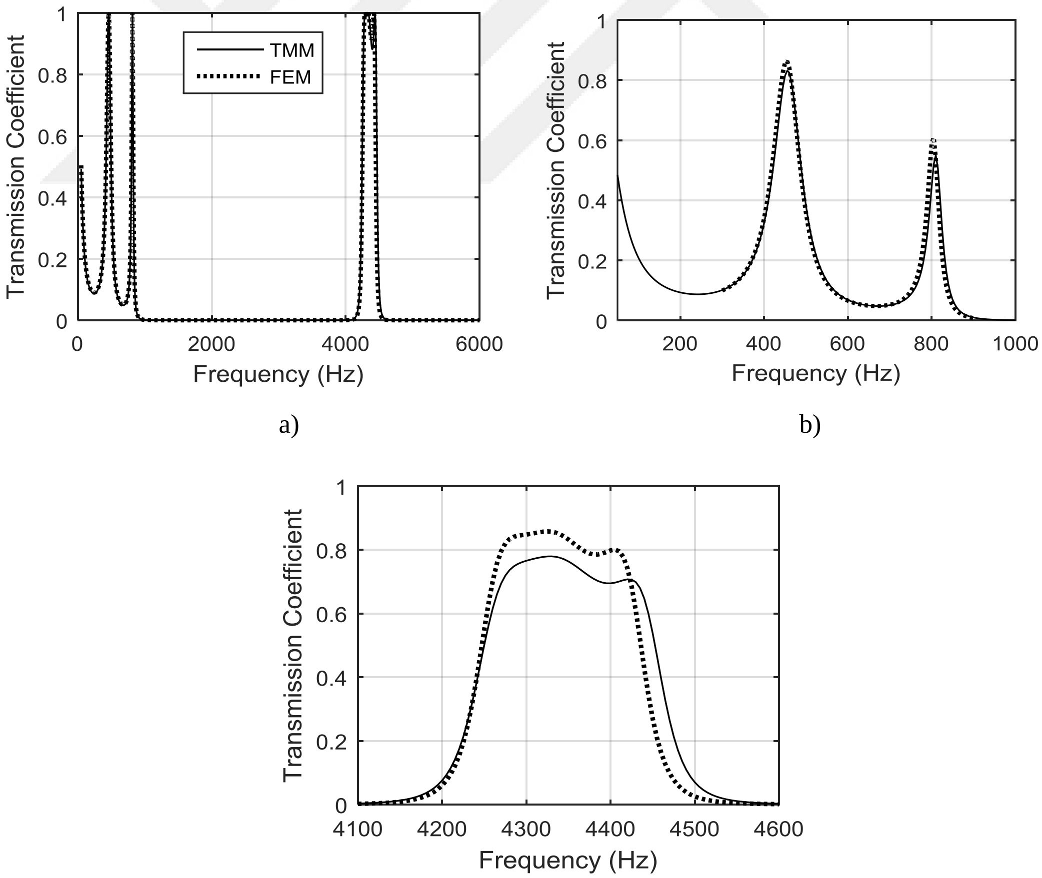

c)

Figure 3.12 Verification of TMM by using FEM for the three-unit case a) without v-t effects, b) with v-t effects (50-1000 Hz), c) with v-t effects (4100-4600 Hz)

Fig 3.11.a presents a perfect match between the TMM and the FEM when v-t effects are neglected. The first peak corresponds the first plane wave mode of the expansion chamber analytically at $f = mc/2L = 4287.5$ Hz (where m=1) which is consistent with the FEM and TMM results. Besides, Fig 3.11.b shows very close results of TMM and FEM with v-t effects. The similar behaviours are also seen for the material with three-unit cases as shown in Fig 3.12. However, there are small discrepancies especially at higher frequency peaks in case of v-t effects are taken into consideration; this may be caused due to the differences of analytical and numerical v-t models adapted.

3.2.2.3 The effect of cellular periodicity

In this section, the effect of cellular arrangement of an acoustic transmission line metamaterial on the acoustic performance parameters is investigated by using TMM in case of visco-thermal effects are taken into account. For this purpose three different cellular arrangements, each of which have the same total expansion volume but changeable diameters, are designed. These metamaterials are composed of four circular expansion chamber type units as schematically shown in Fig. 3.8. The arrangements are made by changing the diameters of expansion; i) cells with the same expansion diameters ("mean"), ii) cells with golden-ratio increasing diameters ("golden ratio") and iii) cells with linearly increasing diameters ("linear"). Table 3.2 tabulates the diameters of expansions.

Table 3.2 Diameters of expansion of considered metamaterials shown in Fig. 3.8 with noting that a=12.5 mm, b=5 mm, L=40 mm for each cell

Cellular Arrangements	d_1 (mm)	d_2 (mm)	d_3 (mm)	d_4 (mm)
Arr. 1 (Mean)	53.904	53.904	53.904	53.904
Arr. 2 (Golden Ratio)	20.225	32.724	52.947	85.669
Arr. 3 (Linear)	25.254	42.091	58.928	75.765
Total volume of expansion	3.6513×10^5 mm^3			

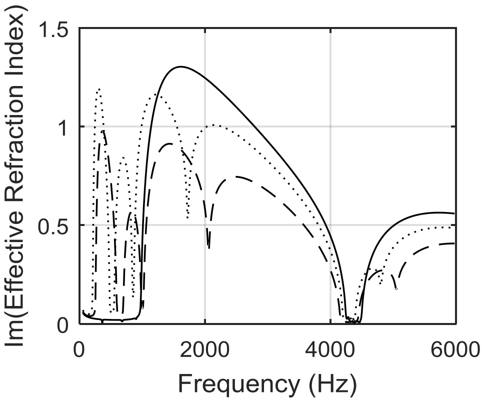

a)

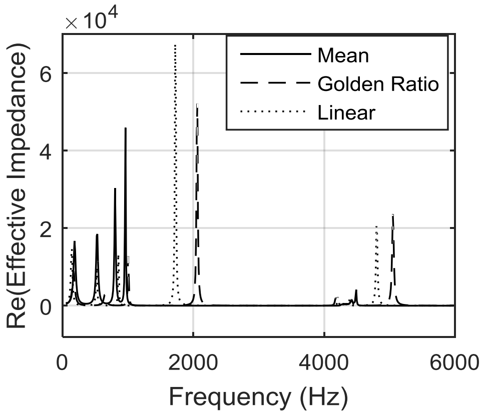

b)

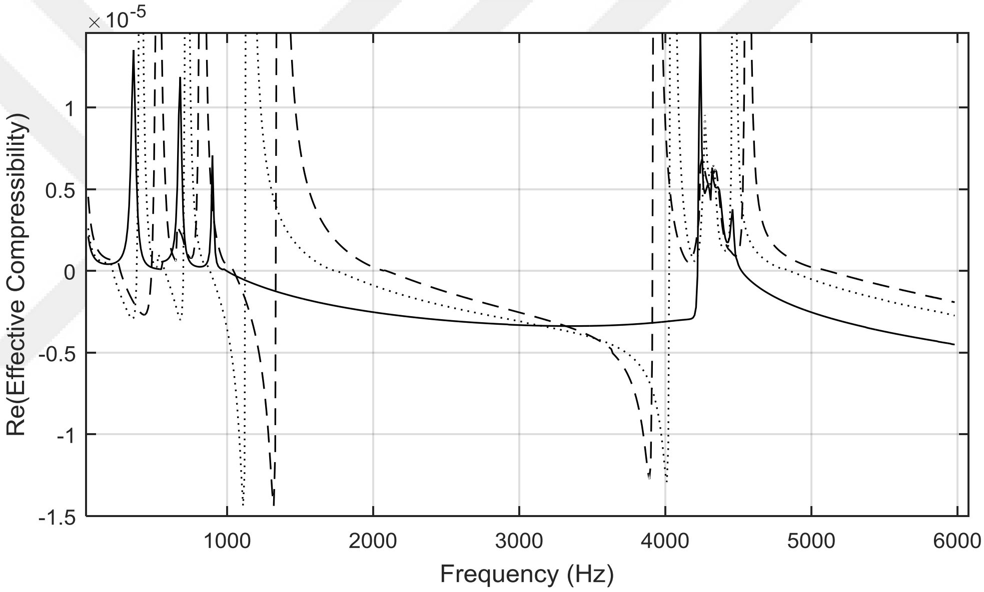

c)

Figure 3.13 Effective parameters of three metacells arrangements: a) Imaginary part of effective refraction indices, b) Real part of effective impedances, c) Real part of effective compressibility

Here, the analyses start with determining effective medium parameters of the metamaterial arrangements. It is known for a passive medium that, the conditions $\mathrm{imag}(n_{eff}) \geq 0$ and $\mathrm{real}(Z_{eff}) \geq 0$ must be satisfied for physical consistency. Fig 3.13.a and b show that all three arrangements satisfy essential physical consistencies. Besides, Fig 3.13.c presents that those materials exhibit negative compressibility at certain frequency bands. This property states that these materials are considered as "metamaterial".

In Fig. 3.14, all three arrangements are compared by themselves and with a single cell having the same total expansion volume. At first glance, it is seen that total volume bans the transmission of waves up to about 4000 Hz. This exhibits a pure reflective character of a single cell. However, the other arrangements let the waves transmit at certain frequencies called F-P frequencies. These behaviours improve absorption characteristics of periodic metamaterials as shown in Fig. 3.15, which is a required property from a metamaterial if they are specifically designed as an absorption material.

When Fig. 3.14 and Fig. 3.15 are investigated in detail, following conclusions can be drawn;

- The peaks up to 1000 Hz are caused due to Fabry-Perot frequencies and improve absorption around those peaks.
- A stop-band behaviour is observed between about 1000-4000 Hz. This shows that the materials exhibit a band pass filter.
- The peaks observed at 4000-4600 Hz show the resonance behaviour of each unit cells. This behaviour also improves absorption.
- Absorption limit is obtained as 0.5, as expected, since these kind of materials (single negative, cavity based) shows monopole behaviour. “Mean” composition shows higher absorption values, however “golden ratio” composition have wider bandwidth.
- When considering higher absorption and wider bandwidth together, it seems that the best choice is “linear” composition.
- “Linear” composition also seems as the best choice among others for the transmission loss character, if one expects small transmission and higher absorption at a wide band.

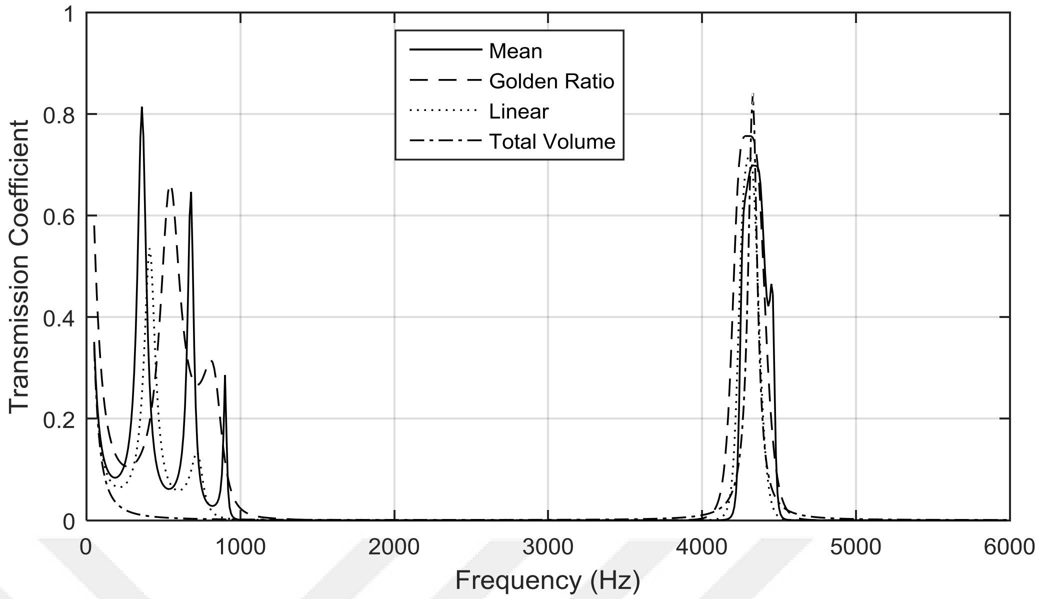

Figure 3.14 Transmission coefficients of different cellular arrangements

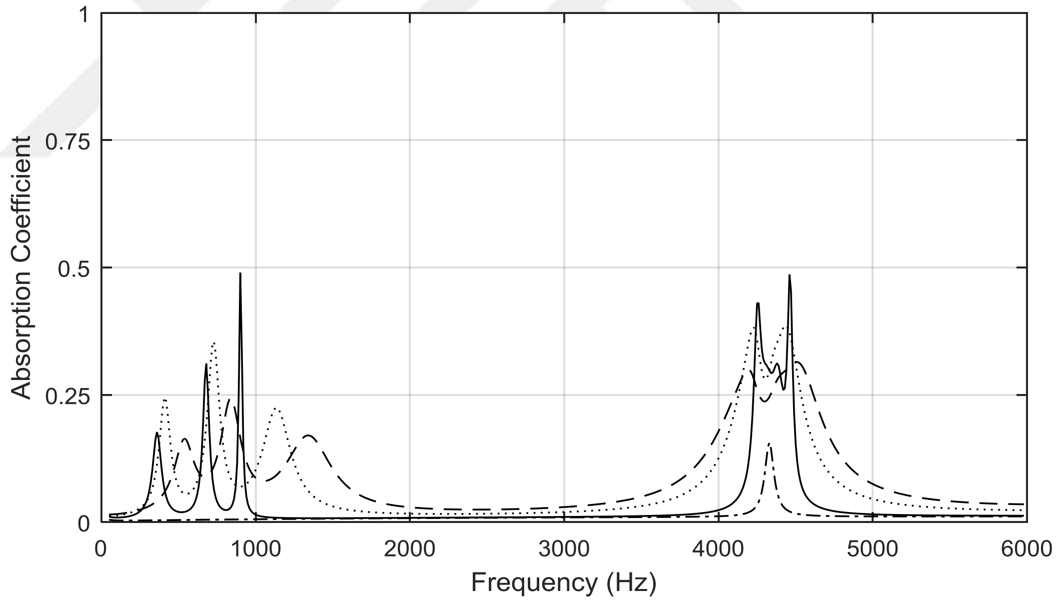

Figure 3.15 Absorption coefficients of different cellular arrangements

CHAPTER FOUR
DESIGN OF PANEL TYPE ACOUSTIC METAMATERIALS

4.1 Introduction

This section is devoted to the design and analyses of panel type acoustic metamaterials. Although the designs have been made for panel type absorbers, the geometries are made as circular shape in order to be used in the standard impedance tube measurements. Here three different models are designed and are manufactured via 3D printing as shown in Fig. 4.1. Experimental measurements for sound absorption and transmission have been performed for these designs. The thickness of each material is limited as 3.8 cm.

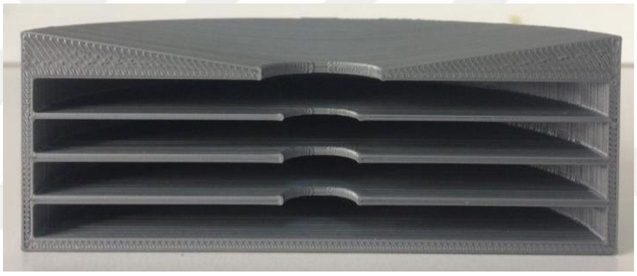

a)

b)

c)

Figure 4.1 3D printed models a)Model 1, b)Model 2, c)Model 3 (Personal archive, 2019)

4.2 Experimental Studies

In this section, sound absorption and transmission coefficients of three different models shown in Fig.4.1 are determined via two microphone method and two load method, respectively. These two methods are standardized based on transfer function method. Details of these methods are given in the following sections.

4.2.1 Sound Absorption Coefficient Measurements via Two Microphone Method

4.2.1.1 Methodology

According to ISO 10534-2: 1998 (E), an impedance tube kit is arranged as shown in Fig 4.2.

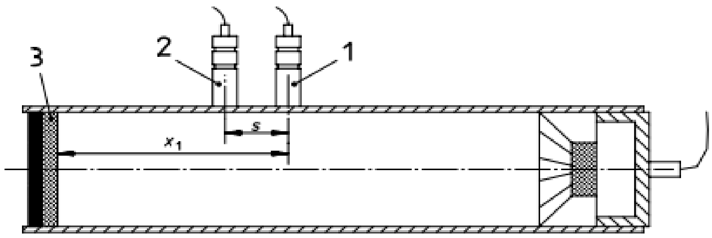

Figure 4.2 Two microphone method experiment arrangement (ISO 10534-2: 1998 (E))

The measurement procedure of two microphone method is based on transfer function method. The reflection coefficient can be computed by using the measured sound pressures via microphone 1 and 2 as (ISO 10534-2: 1998 (E))

$$R(\omega) = |R| e^{j\phi_R} = \frac{H_{12}(\omega) - H_i}{H_r - H_{12}(\omega)} e^{2jk_0 x_1} \tag{4.1}$$

where H_{12}, H_i and H_r are cross spectral transfer function of microphone 1 and microphone 2, incident wave and reflected wave transfer functions, respectively, x_1 is the distance between microphone 1 and sample as shown in Fig. 4.2. Note that p_1

and p_2 are complex acoustic pressures and overbar indicates their complex conjugates. These transfer functions are computed as

$$H_{12}(\omega) = \frac{p_2 \cdot \bar{p}_1}{p_1 \cdot \bar{p}_1}, \tag{4.2}$$

$$H_i = e^{-jks}, \tag{4.3}$$

$$H_r = e^{jks}, \tag{4.4}$$

where *s* is the distance between the microphones and should be selected as providing following condition;

$$s < \frac{0.45c}{f_u}. \tag{4.5}$$

Here f_u is the upper limit of the measurement frequency range. Then sound absorption coefficient is obtained as

$$\alpha(\omega) = 1 - |R(\omega)|^2, \tag{4.6}$$

4.2.1.2 Experimental Results

In this section, sound absorption coefficients of three metamaterials and three different passive materials shown in Fig. 4.3 are measured based on the instructions of the standard given in the previous section. Note that only metamaterial model 1 is presented in Figure 4.3. Table 4.1 presents mass densities and thicknesses of each material.

a) b) c) d)

Figure 4.3 Passive materials a) Passive a: Fiber-glass, b) Passive b: Foam, c) Passive c: Dense Foam, d) Model 1: Metamaterial (Personal archive, 2019)

Table 4.1 Physical properties of the passive materials

Material	Density (kg/m^3)	Thickness (mm)
Passive a: Fiber-glass	50	43
Passive b: Foam	80	35
Passive c: Dense Foam	120	46
Metamaterial all models	-	38

Repeatability tests of the passive materials and the metamaterials are given in Figs. 4.4 and 4.5, respectively. These figures show that measurements are consistent and reliable.

Fig. 4.6 presents a comparison study for sound absorptions of all six materials (three passive, three metamaterials). The passive models exhibit higher absorption as the frequency increases, as expected. It is clearly observed that even though all materials have almost similar thicknesses, the metamaterial models show perfect absorption at some specific low frequencies. This superior absorption is due to the dipole resonances of the plates backed by an acoustic cavity constructing the metamaterial.

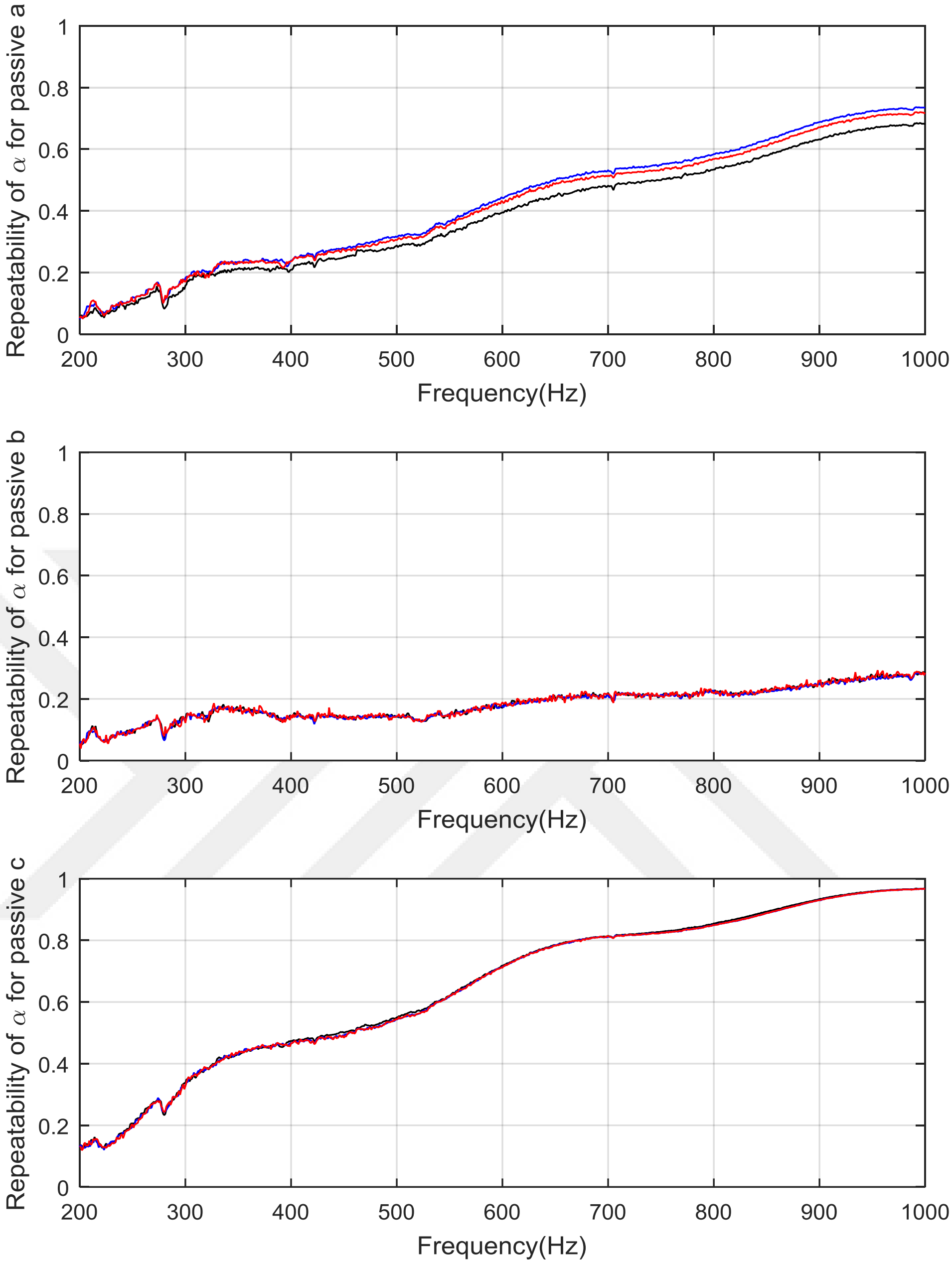

Figure 4.4 Repeatability of absorption coefficients of passive materials

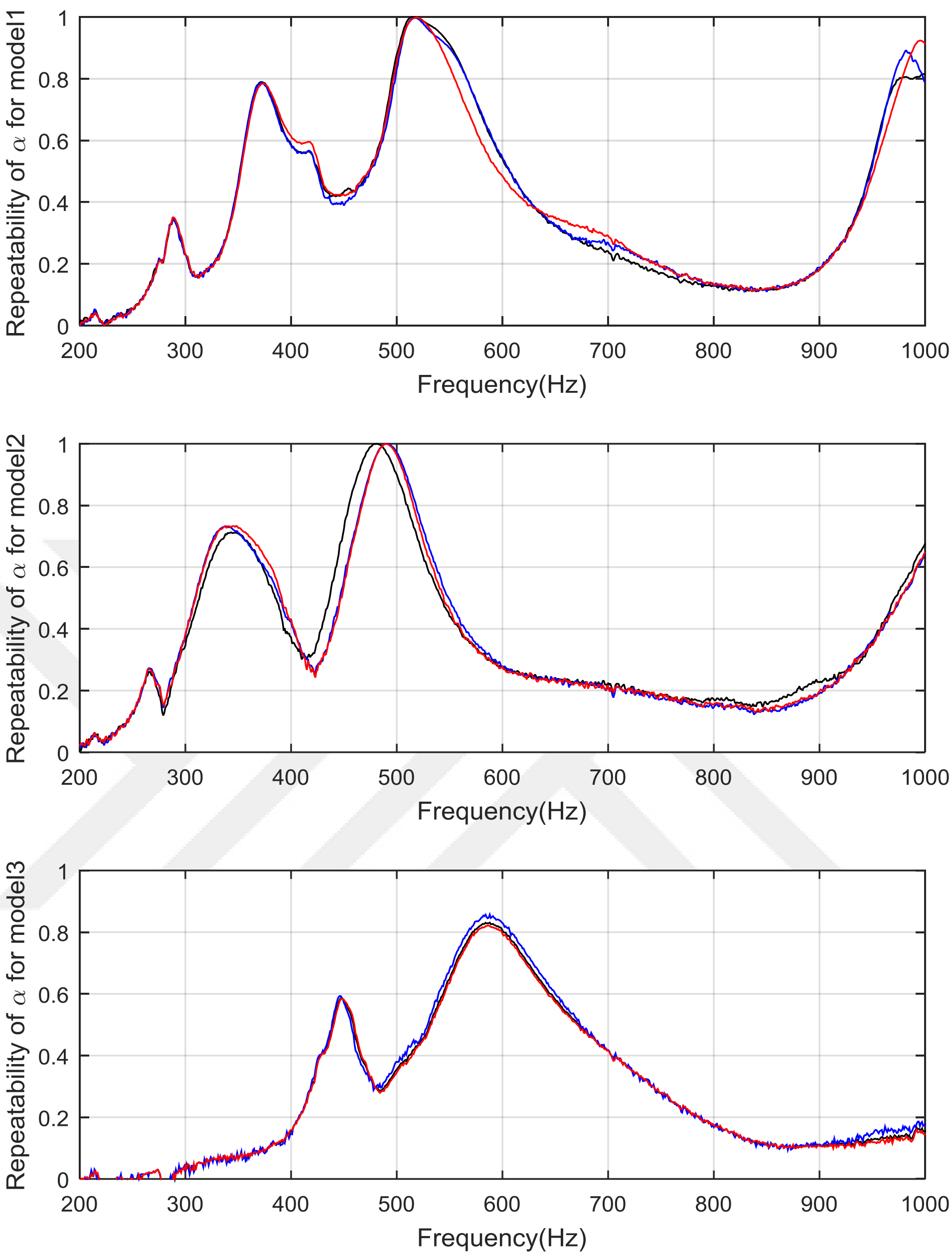

Figure 4.5 Repeatability of absorption coefficients of metamaterial models

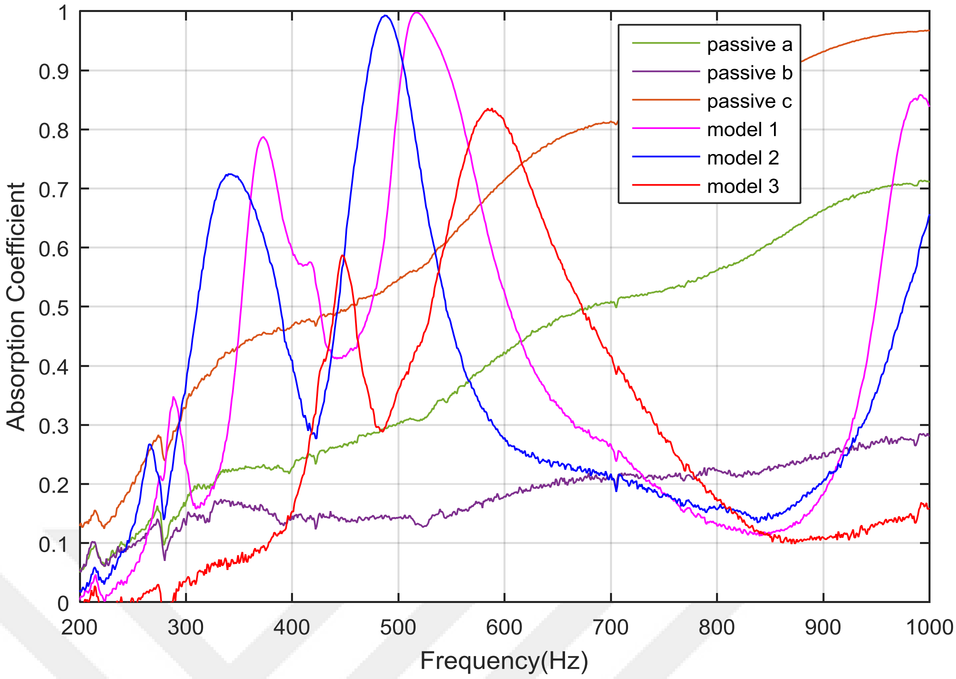

Figure 4.6 Comparison of absorption coefficients of metamaterial models and passive materials

The interaction between the plate and acoustic cavity broadens the absorption spectra around these resonance frequencies. When these models are compared among themselves, it is seen that the model 3 is less efficient. This is probably because of the increasing inner radius, creating higher transmission. Perfect (full) absorptions are observed at 487 Hz for model 2 and 516 Hz for model 1. These frequencies respectively correspond to $d \approx \dfrac{c}{4 \cdot f}$ = 17cm and 16.6 cm thicknesses for a perfect passive material. However, these values are achieved by designed metamaterials with only 3.8 cm thickness. These results indeed state that the main objective of the present thesis is successfully achieved.

4.2.2 Transmission Coefficient Measurements via Two Load Method

4.2.2.1 Methodology

According to the two-load method, transfer matrix elements of test specimen are obtained by measuring two complex pressure response functions ($H_{ij} = P_i / P_j$) at either side of considered structures as shown in Figure 4.7 for each load. In the measurements, the tube end must be any two of hard end, soft end, anechoic end or an impedance end.

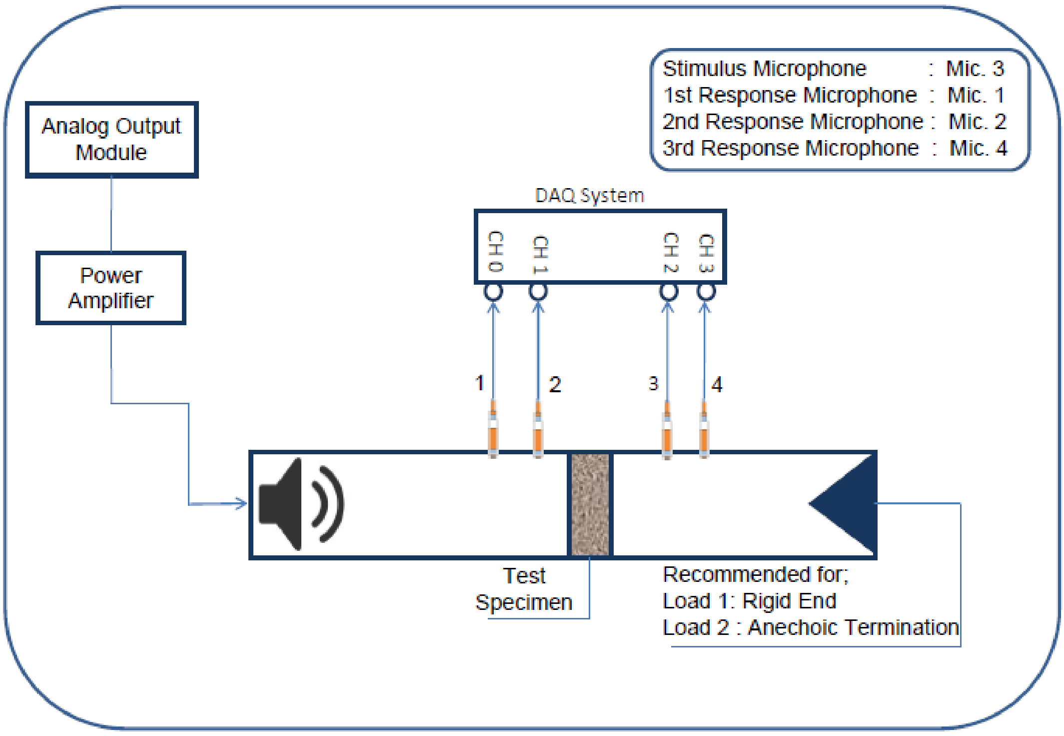

Figure 4.7 Experimental setup of two-load method (İhtiyaroğlu, 2018)

Transfer matrix elements are calculated by determining sound pressures and particle velocities of the test specimen at the inlet and outlet for each load as follows:

$$p_0 = A + B\,, \tag{4.7}$$

$$p_d = Ce^{-jkd} + De^{jkd}\,, \tag{4.8}$$

$$u_0 = (A - B)/Z_0\,, \tag{4.9}$$

$$u_d = \left(Ce^{-jkd} - De^{jkd}\right)/Z_0\,. \tag{4.10}$$

Here, d is the thickness of test specimen, A, B, C and D are forward and backwards travelling wave amplitudes on either side of test specimen and can be calculated by using complex sound pressure response functions (ASTM International, 2009):

$$A = j\frac{H_{13}e^{-jkl_1} - H_{23}e^{-jk(l_1+s_1)}}{2\sin(ks_1)}, \tag{4.11}$$

$$B = j\frac{H_{23}e^{jk(l_1+s_1)} - H_{13}e^{jkl_1}}{2\sin(ks_1)}, \tag{4.12}$$

$$C = j\frac{H_{33}e^{jk(l_2+s_2)} - H_{43}e^{jkl_2}}{2\sin(ks_2)}, \tag{4.13}$$

$$D = j\frac{H_{43}e^{-jkl_2} - H_{33}e^{-jk(l_2+s_2)}}{2\sin(ks_2)}. \tag{4.14}$$

Here, l_1 and l_2 are distances of 2nd and 3rd microphones to the inlet of specimen, $\mathbf{s}_1$ and s_2 are the distance between microphones. One can determine transfer matrix elements by using Eq. (4.7)-(4.10) as follows (ASTM International, 2009):

$$T_{11} = \frac{p_{0a}u_{db} - p_{0b}u_{da}}{p_{da}u_{db} - p_{db}u_{da}} \quad , \tag{4.15}$$

$$T_{12} = \frac{p_{0b}p_{da} - p_{0a}p_{db}}{p_{da}u_{db} - p_{db}u_{da}}, \tag{4.16}$$

$$T_{21} = \frac{u_{0a}u_{db} - u_{0b}u_{da}}{p_{da}u_{db} - p_{db}u_{da}}, \tag{4.17}$$

$$T_{22} = \frac{p_{da}u_{0b} - p_{db}u_{0a}}{p_{da}u_{db} - p_{db}u_{da}}. \tag{4.18}$$

Finally, transmission coefficient can be calculated by using Eq. (2.43) utilizing Eqs. (4.15)-(4.18).

4.2.2.2 Numerical and Experimental Results

Here transmission coefficients of three metamaterial models are numerically and experimentally determined. Repeatability tests of the transmission coefficient measurements are given in Fig. 4.8, whereas the comparision study is presented in Fig. 4.9.

It is observed that there are some discrepancies between experimental and numerical results. However especially for Model 1, the first and the third peaks are very consistent. For the other models, those peaks seem very close to each other as far as frequency characteristic concerns. Although the numerical model is conducted on taking structural-acoustic interaction into account, which makes the analysis more realistic, the difference between the results is probably caused by improper definition of material and geometric properties of metamaterial models in numerical computations.

When the transmission coefficients of three models are compared among themselves, it is also said that the models 1 and 2 are more efficient. However all three models presents different low and high frequency band gaps.

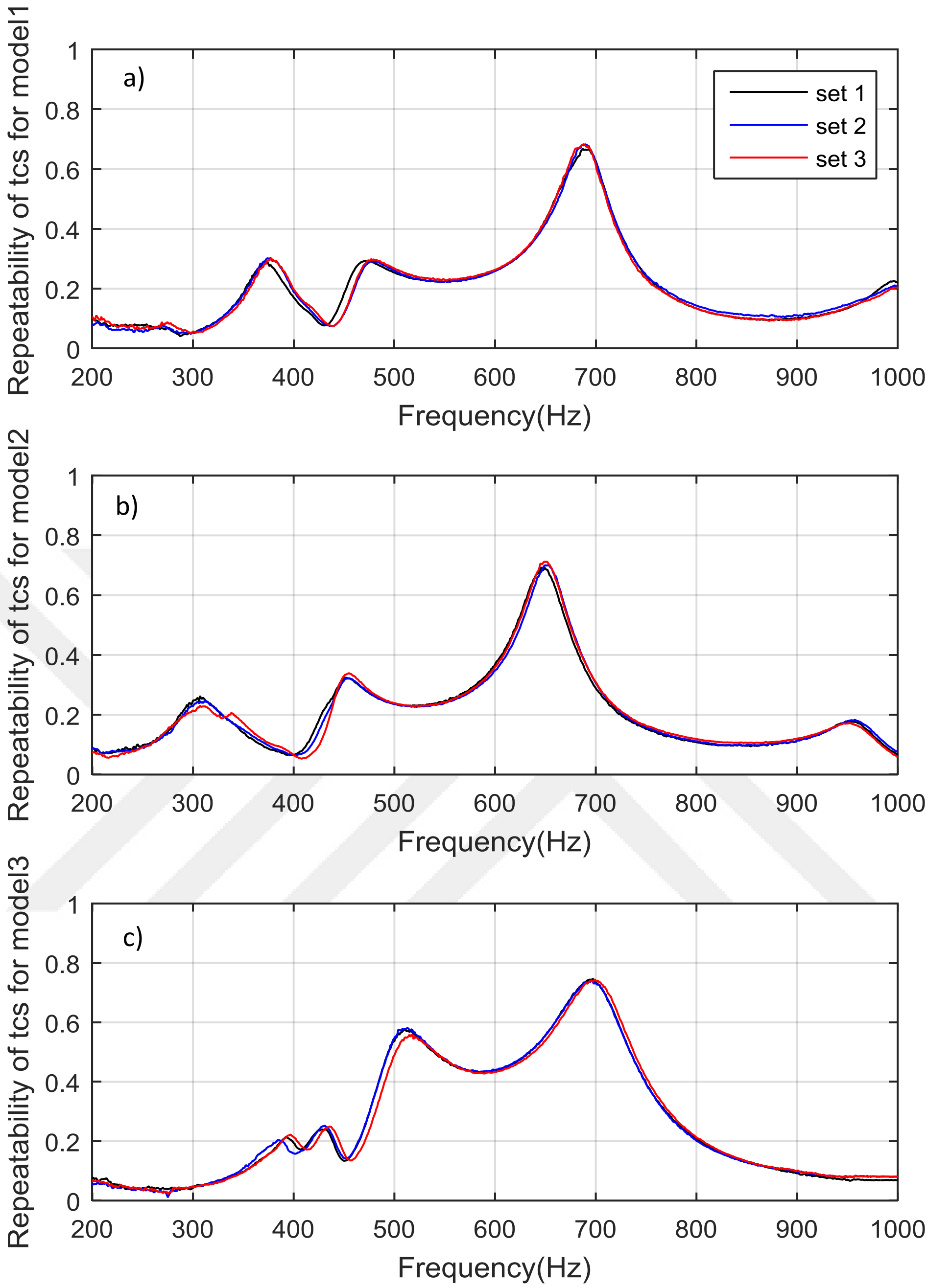

Figure 4.8 Repeatability of transmission coefficients of a) Model 1, b) Model 2, c) Model 3

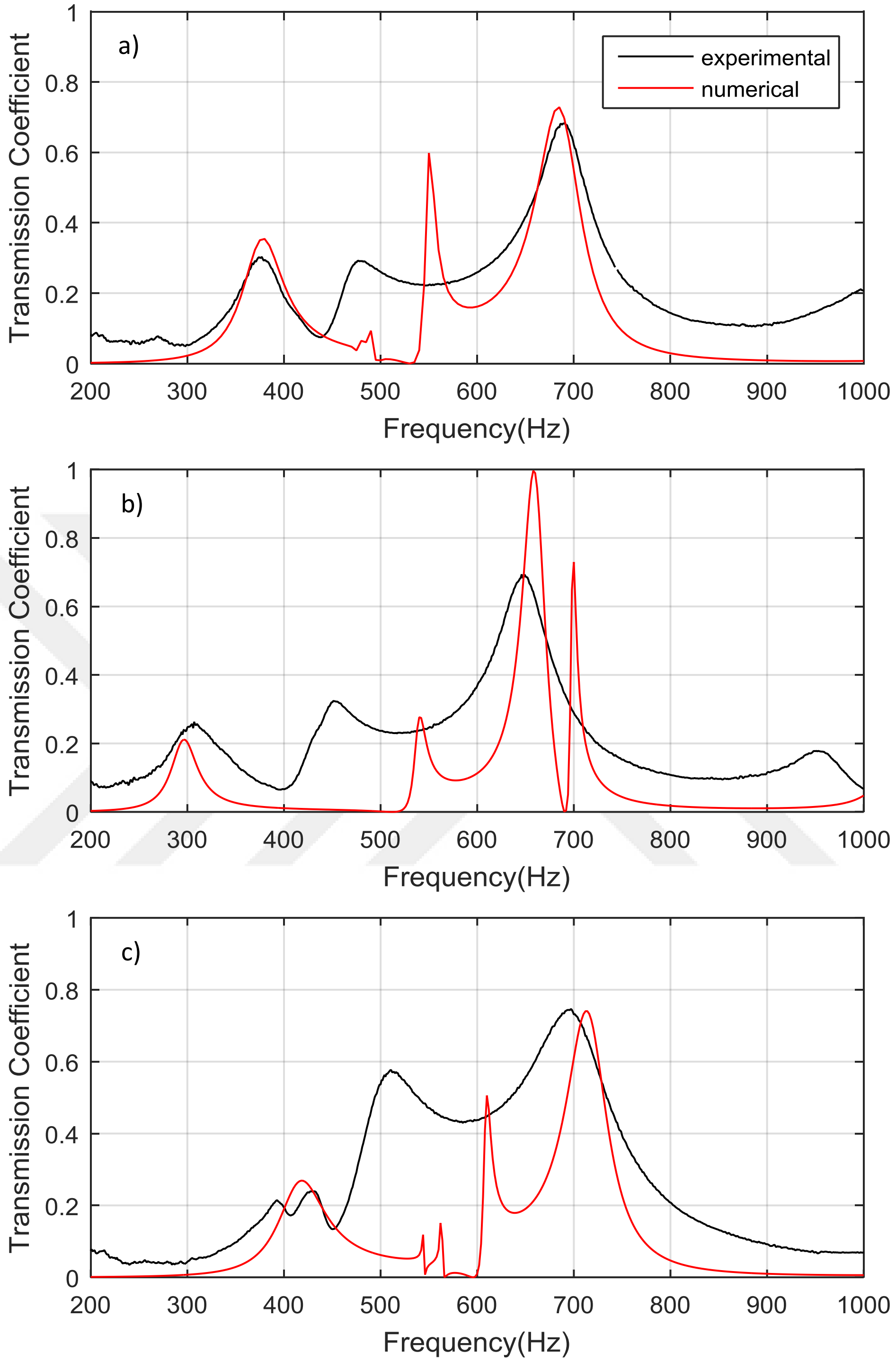

Figure 4.9 Transmission coefficients of a) Model 1, b) Model 2, c) Model 3

CHAPTER FIVE
CONCLUSION

5.1 Thesis Summary

The thesis mainly deals with designing of highly absorptive acoustic metamaterials (AMMs) for low frequency noise suppression. Besides it concerns with transmission characteristics with band gap behaviours. In this scope, several different kinds of AMMs are designed for the acoustic transmission lines and panel type absorbers. The thesis includes a brief but comprehensive literature survey about acoustic metamaterials and related issues on the performance evaluation of those AMMs.

The thesis also presents effective medium homogenization scheme based on transfer matrix method (TMM) to exhibit meta behaviours of these AMMs, and compare them with the conventional passive materials. In this respect, the details on a procedure of retrieving effective medium parameters such as effective refraction index, impedance, mass and compressibility, are introduced.

The analyses for acoustic transmission lines AMMs are performed by finite element method (FEM) and TMM. Visco-thermal (v-t) effects are included in these analyses. One can also find a very useful comparison between analytical v-t models in the thesis. For panel type absorbers, performance parameters are experimentally computed by using an impedance tube kit. Interested readers can also find the theory behind and instructions about these experiments in the thesis.

5.2 Thesis Highlights and Achievements

As it is indicated in the previous section of this Chapter, there are numerous designs and analyses are performed for AMMs. Now it is useful to give here remarkable findings and outcomes of analyses performed in the studies;

- TMM is very successful in the prediction of effective medium parameters of AMMs,

- v-t effects cannot be disregarded especially for narrow and small acoustic cavities,

- Analytical v-t models are very efficient in the prediction of losses in cavities,

- Subwavelength transmission line AMMs can create wide band gaps and allows one to create tuneable band pass filters,

- Plate-cavity interacted metamaterials can create perfect absorption with a wide absorption band,

- The AMMs designed in the thesis study showed that a material with only 38 mm thickness can achieve full absorption at which a perfect passive material with 170 mm thickness may have.

The thesis has made and will make following contributions to the literature;

- Seçgin, A., & Baygün, T. (2019). Determination of effective medium parameters of an in-line cavity based acoustic metamaterials with visco-thermal losses. Materials Research Express, 6(6), 065801.

- Seçgin, A., & Baygün, T. (2019). İç Boşluklu Akustik Metamalzemelerin Homojenizasyonu ve İletim Kayıplarının Transfer Matris Metodu ile Belirlenmesi. Dokuz Eylül Üniversitesi Mühendislik Fakültesi Fen ve Mühendislik Dergisi, 21(62), 449–459.

- Seçgin, A, Baygün T, “Experimental effective medium homogenization of an acoustic metamaterial panel absorber”, In preparation.

- Seçgin, A, Baygün T, “The effect of cellular periodicity on band-gap behaviour of acoustic transmission line metamaterials”, In preparation.

5.3. Future Works

The designs and analyses during the thesis ignited the following ideas and future works;

- AMMs designs can be more effective by a shape optimization based on design objective parameter, i.e., topological optimization required for maximum efficiency.

- AMMs designs can be enhanced and adapted to proper mass production to become commercial products.

- Passive materials are effective on high frequencies and exhibit wider and smoothened bands; therefore they may be combined with AMMs in accordance with the aim of the final product.

- A reliable effective medium homogenization procedure fed by experimental transfer matrices can be developed.

REFERENCES

Alonso-Redondo, E., Schmitt, M., Urbach, Z., Hui, C. M., Sainidou, R., Rembert, P., Matyjaszweski, K., Bockstaller, M. R., Fytas, G. (2015). A new class of tunable hypersonic phononic crystals based on polymer-tethered colloids. *Nature Communications, 6*(1), 8309.

Ambati, M., Fang, N., Sun, C., & Zhang, X. (2007). Surface resonant states and superlensing in acoustic metamaterials. *Physical Review B, 75*(19), 195447.

ASTM International. (2009). *ASTM E2611-09: Standard test method for measurement of normal incidence sound transmission of acoustical materials based on the transfer matrix method.*

Beltman, W. M. (1998). *Viscothermal wave propagation including acousto-elastic interaction.* PhD Thesis, University of Twente, Netherland.

Bongard, F., Lissek, H., & Mosig, J. R. (2010). Acoustic transmission line metamaterial with negative/zero/positive refractive index. *Physical Review B, 82*(9), 094306.

Brillouin, L. (2003). *Wave propagation in periodic structures: electric filters and crystal lattices* (2nd ed.). New York: Dover Publications.

Chen, X., Grzegorczyk, T. M., Wu, B.-I., Pacheco, J., & Kong, J. A. (2004). Robust method to retrieve the constitutive effective parameters of metamaterials. *Physical Review E, 70*(1), 016608.

Chen, Y., & Wang, L. (2014). Periodic co-continuous acoustic metamaterials with overlapping locally resonant and Bragg band gaps. *Applied Physics Letters, 105*(19), 191907.

Cheng, Y., Xu, J. Y., & Liu, X. J. (2008). One-dimensional structured ultrasonic metamaterials with simultaneously negative dynamic density and modulus. *Physical Review B, 77*(4), 045134.

Cheng, Ying, Yang, F., Xu, J. Y., & Liu, X. J. (2008). A multilayer structured acoustic cloak with homogeneous isotropic materials. *Applied Physics Letters, 92*(15), 151913.

Cordioli, J. A., Martins, G. C., Jordan, R., Cordioli1, J. A., Martins1, G. C., Mareze1, P. H., & Jordan1, R. (2010). A comparison of models for visco-thermal acoustic problems. *Internoise 2010, Lisbon, Portugal*, 1–10.

Croënne, C., Lee, E. J. S., Hu, H., & Page, J. H. (2011). Band gaps in phononic crystals: Generation mechanisms and interaction effects. *AIP Advances, 1*(4), 041401.

Cselyuszka, N. (2015). *Novel metamaterial structures for non-conventional propagation of acoustic waves.* PhD Thesis, University of Novi Sad, Serbia.

Cummer, S. A., Christensen, J., & Alù, A. (2016). Controlling sound with acoustic metamaterials. *Nature Reviews Materials, 1*(3), 16001.

Cummer, S. A., Popa, B.-I., Schurig, D., Smith, D. R., Pendry, J., Rahm, M., & Starr, A. (2008). Scattering theory derivation of a 3D acoustic cloaking shell. *Physical Review Letters, 100*(2), 024301.

Deymier, P. A. (2013). *Acoustic metamaterials and phononic crystals* (1st ed). Berlin Heidelberg: Springer-Verlag.

Ding, Y., Liu, Z., Qiu, C., & Shi, J. (2007). Metamaterial with simultaneously negative bulk modulus and mass density. *Physical Review Letters, 99*(9), 093904.

Fahy, F. (2001). *Foundations of Engineering Acoustics.* London: Elsevier Academic Press.

Fang, N., Xi, D., Xu, J., Ambati, M., Srituravanich, W., Sun, C., & Zhang, X. (2006). Ultrasonic metamaterials with negative modulus. *Nature Materials*, *5*(6), 452–456.

Farhat, M., Guenneau, S., Enoch, S., & Movchan, A. B. (2009). Cloaking bending waves propagating in thin elastic plates. *Physical Review B, 79*(3), 033102.

Fokin, V., Ambati, M., Sun, C., & Zhang, X. (2007). Method for retrieving effective properties of locally resonant acoustic metamaterials. *Physical Review B, 76*(14), 144302.

Gebrekidan, S. B., Kim, H.-J., & Song, S.-J. (2019). Investigation of Helmholtz resonator-based composite acoustic metamaterial. *Applied Physics A, 125*(1), 65.

Guenneau, S., Movchan, A., Pétursson, G., & Anantha Ramakrishna, S. (2007). Acoustic metamaterials for sound focusing and confinement. *New Journal of Physics*, *9*(11), 399–399.

Haberman, Michael R., & Guild, M. D. (2016). Acoustic metamaterials. *Physics Today*, *69*(6), 42–48.

Haberman, Micheal. R, & Norris, A. N. (2016). Acoustic metamaterials. *Acoustics Today*, *12*(3), 31–39.

Hirsekorn, M., Delsanto, P. ., Batra, N. ., & Matic, P. (2004). Modelling and simulation of acoustic wave propagation in locally resonant sonic materials. *Ultrasonics, 42*(1–9), 231–235.

Hu, X., Ho, K.-M., Chan, C. T., & Zi, J. (2008). Homogenization of acoustic metamaterials of Helmholtz resonators in fluid. *Physical Review B, 77*(17), 172301.

Huang, H. H., Sun, C. T., & Huang, G. L. (2009). On the negative effective mass density in acoustic metamaterials. *International Journal of Engineering Science, 47*(4), 610–617.

Hussein, M. I., Leamy, M. J., & Ruzzene, M. (2014). Dynamics of phononic materials and structures: Historical origins, recent progress, and future outlook. *Applied Mechanics Reviews, 66*(4), 040802.

İhtiyaroğlu, Y. (2018). *Determination of acoustic of performance parameters of insulation materials in conditioned medium.* MSc Thesis, Dokuz Eylül University, İzmir.

ISO. (1998). *ISO 10534-2:1998(en), Acoustics — Determination of sound absorption coefficient and impedance in impedance tubes — Part 2: Transfer-function method*. (n.d.).

Jiménez, N., Cox, T. J., Romero-García, V., & Groby, J.-P. (2017). Metadiffusers: Deep-subwavelength sound diffusers. *Scientific Reports, 7*(1), 5389.

Joly, N. (2008). Finite element modeling of thermoviscous acoustics in closed cavities. *Acoustics'08 Paris, France,* 2469–2474.

Jung, J. W., Kim, J. E., & Lee, J. W. (2018). Acoustic metamaterial panel for both fluid passage and broadband soundproofing in the audible frequency range. *Applied Physics Letters, 112*(4), 041903.

Kaina, N., Fink, M., & Lerosey, G. (2013). Composite media mixing Bragg and local resonances for highly attenuating and broad bandgaps. *Scientific Reports, 3*(1), 3240.

Kampinga, W. R., Wijnant, Y. H., & de Boer, A. (2010). Performance of several viscothermal acoustic finite elements. *Acta Acustica United with Acustica, 96*(1), 115–124.

Krushynska, A. O., Miniaci, M., Bosia, F., & Pugno, N. M. (2017). Coupling local resonance with Bragg band gaps in single-phase mechanical metamaterials. *Extreme Mechanics Letters, 12*, 30–36.

Lan, J., Li, Y., Yu, H., Li, B., & Liu, X. (2017). Nonlinear effects in acoustic metamaterial based on a cylindrical pipe with ordered Helmholtz resonators. *Physics Letters A, 381*(13), 1111–1117.

Lazarov, B. S., & Jensen, J. S. (2007). Low-frequency band gaps in chains with attached non-linear oscillators. *International Journal of Non-Linear Mechanics, 42*(10), 1186–1193.

Lee, S. H., Park, C. M., Seo, Y. M., Wang, Z. G., & Kim, C. K. (2009a). Acoustic metamaterial with negative density. *Physics Letters A, 373*(48), 4464–4469.

Lee, S. H., Park, C. M., Seo, Y. M., Wang, Z. G., & Kim, C. K. (2009b). Acoustic metamaterial with negative modulus. *Journal of Physics: Condensed Matter, 21*(17), 175704.

Li, J., & Chan, C. T. (2004). Double-negative acoustic metamaterial. *Physical Review E, 70*(5), 055602.

Liu, Z., Zhang, X., Mao, Y., Zhu, Y. Y., Yang, Z., Chan, C. T., & Sheng, P. (2000). Locally resonant sonic materials. *Science, 289*(5485), 1734–1736.

Lu, L., Yamamoto, T., Otomori, M., Yamada, T., Izui, K., & Nishiwaki, S. (2013). Topology optimization of an acoustic metamaterial with negative bulk modulus using local resonance. *Finite Elements in Analysis and Design, 72*, 1–12.

Ma, G., & Sheng, P. (2016). Acoustic metamaterials: From local resonances to broad horizons. *Science Advances, 2*(2), e1501595.

Malinen, M., Lyly, M., Råback, P., Kärkkäinen, A., & Kärkkäinen, L. (2004). A finite element method for the modeling of thermo-viscous effects in acoustics. *Proceedings of the European Congress on Computational Methods in Applied Science and Engineering ECCOMAS 2004, Jyväskylä, Finland,* 1-12.

Mechel, F. P. (2008). *Formulas of acoustics* (2nd ed.). New York: Springer.

Moleron, M., Marc, S.-G., & Daraio, C. (2015). Visco-thermal effects in acoustic metamaterials: From total transmission to total reflection and high absorption. *New Journal of Physics, 18*(3), 033003 1-8.

Movchan, A. B., & Guenneau, S. (2004). Split-ring resonators and localized modes. *Physical Review B, 70*(12), 125116.

Munjal, M. L. (1987). *Acoustics of ducts and mufflers with application to exhaust and ventilation system design.* New York: John Wiley&Sons.

Nicolson, A. M., & Ross, G. F. (1970). Measurement of the Intrinsic Properties of Materials by Time-Domain Techniques. *IEEE Transactions on Instrumentation and Measurement, 19*(4), 377–382.

Peng, L. (2017). Sound absorption and insulation functional composites. *Advanced High Strength Natural Fibre Composites in Construction*, 333–373. United Kingdom: Woodhead Publishing.

Popa, B. I., Zigoneanu, L., & Cummer, S. A. (2011). Experimental acoustic ground cloak in air. *Physical Review Letters, 106*(25), 253901.

Seçgin, A., & Baygün, T. (2019a). Determination of effective medium parameters of an in-line cavity based acoustic metamaterials with visco-thermal losses. *Materials Research Express, 6*(6), 065801.

Seçgin, A., & Baygün, T. (2019b). İç Boşluklu Akustik Metamalzemelerin Homojenizasyonu ve İletim Kayıplarının Transfer Matris Metodu ile Belirlenmesi. *Dokuz Eylül Üniversitesi Mühendislik Fakültesi Fen ve Mühendislik Dergisi, 21*(62), 449–459.

Sharma, B., & Sun, C. (2015). *Acoustic metamaterial with negative modulus and a double negative structure.* 7 Jan 2015, https://arxiv.org/ftp/arxiv/papers/1501/1501.02833.pdf

Sheng, P., Zhang, X. X., Liu, Z., & Chan, C. T. (2003). Locally resonant sonic materials. *Physica B: Condensed Matter, 338*(1–4), 201–205.

Stinson, M. R. (1991). The propagation of plane sound waves in narrow and wide circular tubes, and generalization to uniform tubes of arbitrary cross-sectional shape. *The Journal of the Acoustical Society of America, 89*(2), 550–558.

Szabo, Z., Park, G.-H., Hedge, R., & Li, E.-P. (2010). A unique extraction of metamaterial parameters based on Kramers–Kronig relationship. *IEEE Transactions on Microwave Theory and Techniques, 58*(10), 2646–2653.

Theocharis, G., Richoux, O., García, V. R., Merkel, A., & Tournat, V. (2014). Limits of slow sound propagation and transparency in lossy, locally resonant periodic structures. *New Journal of Physics, 16*(9), 093017.

Tijdeman, H. (1975). On the propagation of sound waves in cylindrical tubes. *Journal of Sound and Vibration, 39*(1), 1–33.

Veselago, V. G. (2005). The electrodynamics of substances with simultaneously negative values of ε and μ. *Soviet Physics Uspekhi, 10*(4), 509–514.

Wang, X., & Mak, C.-M. (2012). Wave propagation in a duct with a periodic Helmholtz resonators array. *The Journal of the Acoustical Society of America, 131*(2), 1172–1182.

Yamamoto, T. (2018). Acoustic metamaterial plate embedded with Helmholtz resonators for extraordinary sound transmission loss. *Journal of Applied Physics, 123*(21), 215110.

Yang, Z., Mei, J., Yang, M., Chan, N. H., & Sheng, P. (2008). Membrane-type acoustic metamaterial with negative dynamic mass. *Physical Review Letters, 101*(20), 204301.

Yao, S., Zhou, X., Hu, G. (2008). Experimental study on negative effective mass in a 1D mass-spring system. *New Journal of Physics, 10*(11pp), 43020.

Zhang, X., & Liu, Z. (2004). Negative refraction of acoustic waves in two-dimensional phononic crystals. *Applied Physics Letters, 85*(2), 341–343.

Zhao, H., Liu, Y., Wang, G., Wen, J., Yu, D., Han, X., & Wen, X. (2005). Resonance modes and gap formation in a two-dimensional solid phononic crystal. *Physical Review B, 72*(1), 012301.

Zhou, X., & Hu, G. (2009). Analytic model of elastic metamaterials with local resonances. *Physical Review B, 79*(19), 195109.

Zwikker, C., & Kosten, C. W. (1949). *Sound absorbing materials.* New York: Elsevier.